D. Building physics and design

Objekttyp: **Group**

Zeitschrift: **IABSE congress report = Rapport du congrès AIPC = IVBH Kongressbericht**

Band (Jahr): **13 (1988)**

PDF erstellt am: **11.09.2024**

DAILY THEME D

Building Physics and Design

Physique des constructions et projet

Bauphysik und Entwurf

Chairman:	K. Gertis, FRG
Technical Adviser:	R. Sagelsdorff, Switzerland
Keynote Lecturers:	E. Cziesielsky, Berlin
	B. Adamsson, Sweden

The theme will be introduced by two Keynote Lecturers and printed in the Post-Congress Report, which will be mailed to the participants after the Congress.

Le thème sera introduit par deux orateurs invités, dont les exposés magistraux seront publiés dans le Rapport Post-Congrès; celui-ci sera envoyé aux participants après le Congrès.

Das Thema wird von zwei eingeladenen Referenten eingeführt, deren Referate im Schlussbericht des Kongresses veröffentlicht werden. Dieser Schlussbericht wird den Teilnehmern nach dem Kongress zugestellt.
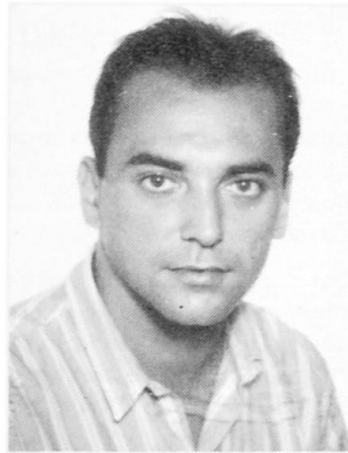
Leere Seite

Blank page

Page vide

Thermal Response of Concrete Box Girder Bridges

Réponse thermique des ponts à poutre-caisson en béton

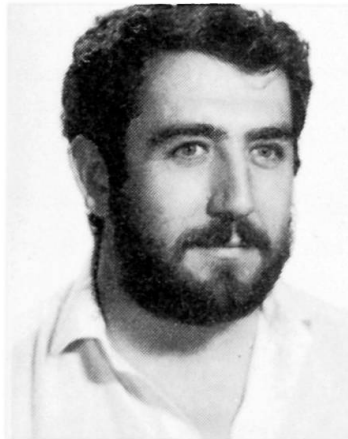Das thermische Verhalten von Betonhohlkastenbrücken

Enrique MIRAMBELL
Assist. Professor
Univ. Politéc. de Cataluna
Barcelona, Spain

Antonio AGUADO
Prof. of Civil Eng.
Univ. Politéc. de Cataluna
Barcelona, Spain

SUMMARY

The present paper is based on the study of environmental thermal effects on concrete box girder bridges. First, we describe the analytical model used to obtain the time-dependent temperature distributions and the selfequilibrated longitudinal and transverse stress distributions. The influence of several factors -environment, physical properties, location of the bridge- on the thermal response of concrete box girder bridges is analyzed. Finally, some recommendations related to the determination of thermal actions to be considered in the design process are suggested.

RÉSUMÉ

L'exposé traite de l'influence des effets climatiques sur les ponts à poutre-caisson en béton armé ou précontraint. Il décrit le modèle analytique des distributions de températures au cours du temps, et les distributions des contraintes dans les directions longitudinale et transversale. Il étudie l'influence de quelques facteurs tels que l'environnement, les propriétés du béton, l'emplacement du pont sur ces distributions. Quelques recommandations pour la détermination de l'action thermique à considérer dans le projet sont faites.

ZUSAMMENFASSUNG

Die thermischen Wirkungen der Umgebung auf Betonbrücken mit Kastenquerschnitt werden untersucht. Es wird zuerst das analytische Modell beschrieben, das wir für das Erzielen der Temperaturverteilungen und der ausgeglichenen Längs-und Querspannungen benutzt haben. Dann wird der Einfluss verschiedener Faktoren — Umgebung, Eigenschaften des Betons, Lage der Brücke – auf die thermische Antwort von Brückenträgern untersucht. Als Folgerung werden einige Empfehlungen für die Festlegung der bei der Bemessung zu berücksichtigenden thermischen Wirkungen gegeben.

1. INTRODUCTION

The interest in reinforced and prestressed concrete bridge analysis and design
in front of environmental thermal effects has increased considerably in recent
years. Measurements in situ have shown that climatic and environmental conditions
were more severe than the ones previously supposed in design. In some cases, this
reason and an inaccurate design in front of thermal loads have induced the appear
ance of cracks in concrete bridges (Ref.[4],[7]).

The present paper is based on the study of environmental thermal effects on con-
crete box girder bridges, at sectional level. In the first place, we describe the
analytical model used to obtain the time-dependent temperature distributions and
the self-equilibrated longitudinal and transverse stress distributions within the
cross-section of concrete box girder bridges. Likewise, the results derived from
several parametric studies are presented.

These results show that strong correlations exist between the annual ambient tem
perature range at the location of the bridge and the annual effective tempera-
ture of the bridge and, also, between the incident solar radiation over the deck
and the thermal imposed curvature. On the other hand, the analytical and experi-
mental results show, in some cases, the importance of thermal horizontal gradi-
ents and thermal transverse loads.

2. ANALYTICAL MODEL

The analytical model used to obtain temperature distributions and stress distribu
tions at sectional level is presented fully in Ref.[6]. However, the bases of the
analysis are described here briefly.

2.1. Temperature distributions

The differential equation that governs the heat transfer problem is

$$div(-\underline{K} \cdot grad\ T) - \dot{q} + \rho c\ \frac{\partial T}{\partial t} = 0 \tag{1}$$

Assuming that concrete verifies several hypotheses -continuum, isotropy and homo
geneity- and that the hardening process has finished, the equation (1) is trans-
formed into

$$\nabla^2 T = \frac{\rho c}{k} \frac{\partial T}{\partial t} \qquad \begin{array}{l} \rho,\ \text{density of concrete} \\ c,\ \text{specific heat} \\ k,\ \text{conductivity} \end{array} \tag{2}$$

The boundary condition at the external surfaces of the deck bridge is the Newmann
condition, which can be expressed in two dimensions as

$$k(\frac{\partial T}{\partial x} n_x + \frac{\partial T}{\partial y} n_y) + aI + (h_c + h_r)(T - T_a) = 0 \tag{3}$$

The analytical model developed to solve the differential equation (2), with the
boundary condition (3), and determine the time-dependent temperature distribu-
tions within the cross-section of concrete box girder bridges is based on two-
dimensional finite difference method. Characteristics of the numerical program de
veloped can be found in Ref.[5]. The convergence and numerical stability condi-
tion is (Ref.[6]).

$$\Delta t \leq \frac{\rho c}{k} \frac{1}{2(\frac{1}{\Delta x^2} + \frac{1}{\Delta y^2}) + \frac{1}{k}(\frac{h_1}{\Delta y} + \frac{h_2}{\Delta x})} \tag{4}$$

2.2. Self-equilibrated stress distributions

Temperature distributions within the cross-section of concrete box girder bridges
are nonlinear. In order to obtain the stress distributions at sectional level,
the Navier-Bernouilli hypothesis is assumed. Due to this fact, self-equilibrated

longitudinal and transverse stresses are induced by temperature distributions in concrete box girder bridges. Such stress distributions are independent of the support conditions of the structure and can be obtained by means of the following equation:

$$\sigma(x,y) = E(\varepsilon_o + \psi_x y + \psi_y x - \alpha T(x,y)_{nl})$$

$$\varepsilon_o = \frac{\alpha}{A}\int\int T(x,y)_{nl} dx\, dy$$

$$\psi_x = \frac{\alpha}{I_x}\int\int T(x,y)_{nl} y\, dx\, dy \qquad (5)$$

$$\psi_y = \frac{\alpha}{I_y}\int\int T(x,y)_{nl} x\, dx\, dy$$

3. INFLUENCE OF SOME PARAMETERS ON THE THERMAL RESPONSE OF CONCRETE BOX GIRDER BRIDGES. ASSOCIATED STRESS DISTRIBUTIONS.

The thermal response of concrete box girder bridges depends on many factors -environmental conditions, structural parameters, physical properties and parameters depending on location of the bridge-. In this chapter, results derived from parametric studies related to several variables are presented and analyzed. The basic study of reference can be seen in Fig. 1 and Table 1. Values of the different parameters are from Ref. [1].

Fig 1. Cross-section and finite
       difference mesh.
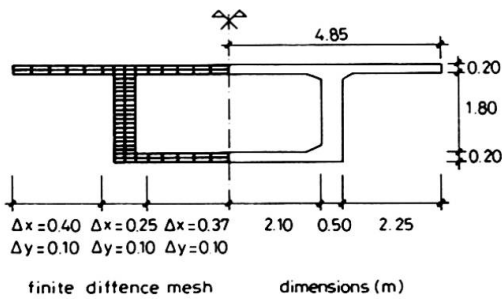
Thermal and structural properties	Thermal diffusivity (m²/h)	0.0023
	Absorbity	0.5
	Emissivity	0.88
	Thermal expansion coef. (°C⁻¹)	8.0x10⁻⁶
	Modulus of elasticity (MPa)	27386.
Environmental conditions	Ambient air temperature (°C)	-5.÷20.
	Wind speed (m/s)	1.0
	Turbidity factor	1.8
	Day of the year	March, 21
Location and orientation of bridge	Latitude (°N)	51.0
	Altitude (m)	1050.
	Azimuth (°)	0.

Table 1. Values of the different parameters in the reference study.

3.1. Influence of solar radiation

The influence of solar radiation intensity on the deck of the bridge may be considered by means of several explicit expressions (Ref. [2]). In this study, the effect of solar radiation is introduced in a general way, depending on several variables. The parameters which show a more significant influence are the day of the year and the latitude of the location of the bridge. The annual evolutions of the maximum vertical and horizontal thermal gradients, maximum daily range of effective temperature of the bridge and maximum temperature differences between the surrounding air and the air enclosed within the cell can be observed in Fig.2. Likewise, the annual evolution of the maximum longitudinal self-equilibrated tensile stress in concrete is presented in Fig.3.

As one can see from both figures, the most unfavourable situation is presented under summer conditions. During this season, nonlinearity of temperature distributions is very marked and, due to this effect, thermal actions and self-equilibrated longitudinal stresses are higher than the ones obtained during other seasons. The critical zones of the cross-section subjected to maximum longitudinal tensile stresses are the webs, while heating the deck, and the extreme fibers and the overhangings, while cooling the deck. Also, it may be interesting to analyze the annual evolution of the horizontal thermal gradient, which reaches the maximum value during the months of winter and it is zero during the months of spring and summer. That is due to the small inclination of the sun's rays with respect to horizontal plane during the winter season.

On the other hand, the influence of latitude must be considered in order to ob-

tain the solar radiation intensity. The maximum thermal imposed curvatures occur under summer conditions, and the higher the latitude, the bigger the curvature produced and the smaller the self-equilibrated stresses induced are.
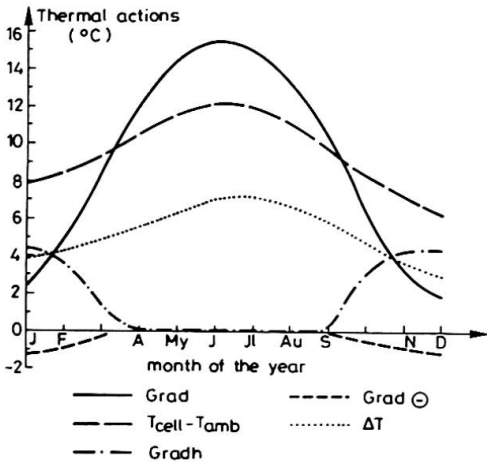

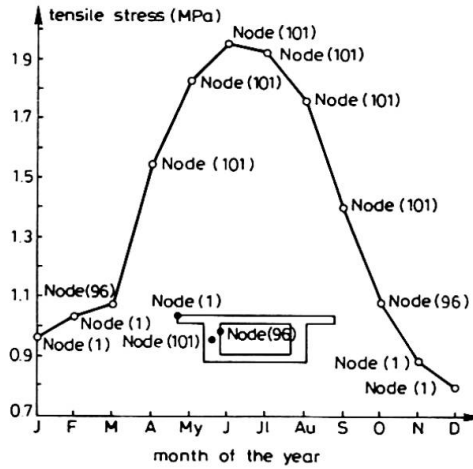
Fig.2. Annual evolutions of different thermal actions.

Fig.3. Annual evolution of the maximum longitudinal tensile stress.

3.2. Influence of asphalt thickness

The presence of asphalt cover on the concrete deck has an influence on the thermal response of concrete bridges due to its different thermal properties. In fact, as one can see from Figs.4 and 5, the presence of asphalt cover with a small thickness results in an increase of the thermal curvatures and the self-equilibrated thermal stresses while the presence of a thicker asphalt cover results in a decrease of the thermal curvatures and the thermal stresses.
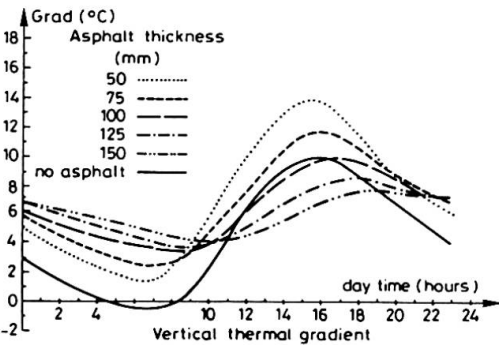
Fig.4. Daily evolution of vertical thermal gradients.
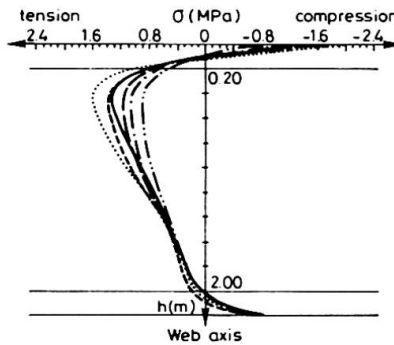
Fig.5. Self-equilibrated longitudinal thermal stresses corresponding to maximum curvatures (web axis).

We may note the existence of a limit asphalt thickness above which the thermal actions and the self-equilibrated thermal stresses are less than their counterpart without asphalt cover. This limit depends on environmental conditions and on superstructure depth. In our case, the limit asphalt thickness is close to 10 cm.

3.3.- Influence of superstructure depth and location of the bridge

Consider a hypothetical prestressed concrete box girder bridge with variable superstructure depth just as the one presented in Fig.6. This hypothetical bridge is located in Barcelona, Spain, in one case, and Helsinki, in the other. The main results derived from both thermal analysis are presented in Table 2. Thermal properties and azimuth are the same of Table 1.

These results show that vertical thermal gradient and daily and annual ranges of effective temperature of the bridge decrease with an increase of superstructure

depth. On the contrary, the minimum horizontal thermal gradient occurs always at midspan cross-section. A comparative analysis of the results obtained in both studies permits to conclude that bridges located at higher latitudes may be subjected to less vertical ther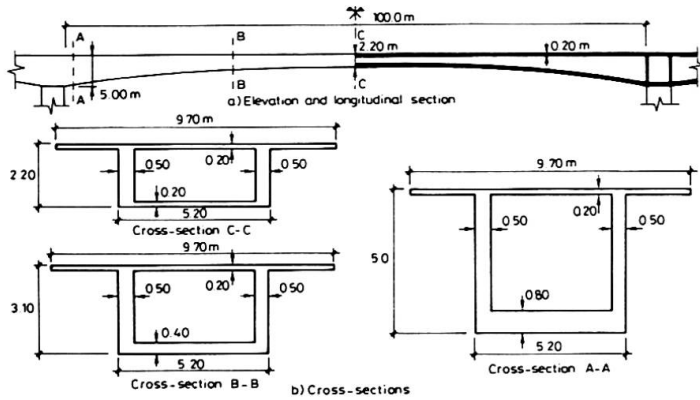mal gradients. However, they are subjected to larger horizontal thermal gradients due to the small inclination of the sun's rays.

Fig.6. Elevation and longitudinal section of the bridge. Cross-sections.

In any case, it is interesting to point out that the horizontal thermal gradient and the temperature difference between the surrounding air and the air enclosed within the cell are significative. The effects produced by these thermal actions could be a source of cracks in concrete box girder bridges and, in general, have not been considered in design. Such results have already been indicated in several experimental analysis (Ref.[3]).

Location of the bridge	Thermal actions (°C)	Cross-section A-A		Cross-section B-B		Cross-section C-C	
		March, 21	June, 10	March, 21	June, 10	March, 21	June, 10
Barcelona	Grad	5.2	5.9	5.8	6.8	6.4	7.4
Latitude 41.4°N	Gradh	2.1	0.	0.5	0.	0.	0.
Altitude 100 m	ΔT	2.5	2.5	3.2	3.5	4.1	4.6
Wind speed 5 m/s	$T_{cell}-T_{amb}$	5.1	5.3	5.1	5.7	5.2	5.8
Helsinki	Grad	3.8	5.5	3.9	6.1	4.0	6.5
Latitude 60.1°N	Gradh	4.0	1.1	2.5	0.	1.4	0.
Altitude 100 m	ΔT	2.6	2.9	3.3	3.7	4.0	4.8
Wind speed 5 m/s	$T_{cell}-T_{amb}$	5.6	6.3	5.5	6.6	5.5	6.7

Helsinki, March 21, turb = 2.0, T_{amb} = -9÷-1°C   Barcelona, March 21, turb = 2.0, T_{amb} = 9÷15.7°C
Helsinki, June 10, turb = 3.5, T_{amb} = 10÷19°C   Barcelona, June 10, turb = 3.5, T_{amb} = 18÷25.1°C

Grad = maximum vertical thermal gradient.
Gradh = maximum horizontal thermal gradient.
ΔT = daily range of effective temperature of the bridge.

$T_{cell}-T_{amb}$ = temperature difference between surrounding air and air enclosed within the cell.

Table 2. Results of thermal analysis of the same bridge (Fig.6) located in Barcelona (Spain) and Helsinki (Finland).

4. THERMAL ACTIONS TO BE CONSIDERED IN DESIGN

Starting from the results of existing parametric studies (Ref.[5]), some of them shown in this paper, it may be possible to determine the thermal actions to be considered in design. This will be useful to bridge designers, in order to take into account the environmental thermal effects in the design process, in a simple and realistic way.

Related to annual range of effective temperature of the deck, the results show a strong correlation between this thermal action and the annual ambient temperature range at the location of the bridge. On the other hand, in the study of vertical thermal gradient, the main environmental factor is the solar radiation. However, in this case, the influence of superstructure depth and asphalt thickness are well known and significative. Fig.7 shows, as an example, the map of Spain with the isolines of vertical thermal gradient related to concrete box girder bridges (depth 2.20 m.) located on the Iberian Peninsula.

This map has been ob-.
tained from data pro-
cessing of solar radi
ation, ambient air tem
perature and wind speed,
collected in several
reports of the Meteorol
ogy Institute of Spain.
The values of the ther
mal actions to be con-
sidered in design pre-
dicted by this study
are in good agreement
with the values derived
from temperature con-
trols carried out in
several concrete bridges
located in Spain (Ref.
[5]).

Fig.7. Isolines of vertical thermal gradient on concrete
box girder bridges (depth=2.20 m) located in Spain.
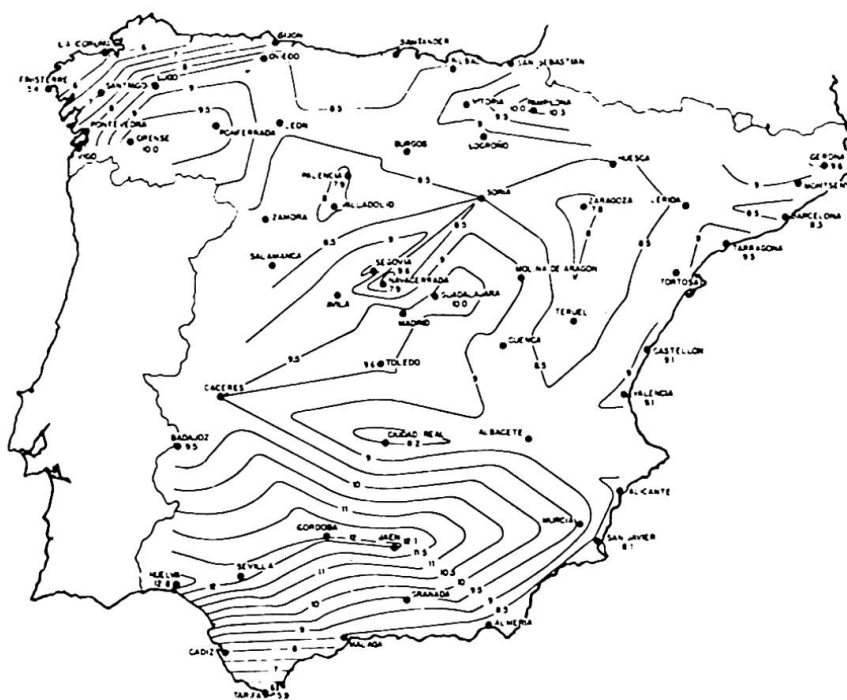
5. CONCLUSIONS

In the first place, en-
vironmental thermal ef-
fects must be considered
in the design process
of concrete box girder bridges and, basically, in serviceability limit state.

The main climatological parameter required to determine the design effective tem
perature range is the annual range of ambient temperature at the location of the
bridge. The main climatological parameter required to determine the design ther-
mal gradient is the solar radiation intensity. In this case, other variables such
as superstructure depth and asphalt thickness must also be taken into account in
design.

The variables which show a greater influence on the horizontal thermal gradient
are the latitude of the location and the azimuth of the bridge and the day of the
year. Depending on these variables, the horizontal thermal gradient can be sig-
nificant   and it must be considered in design.

Finally, the transverse thermal stresses due to nonlinearity of temperature dis-
tributions and temperature difference between the surrounding air and the air en
closed within the cells must be considered in design. Basically, these thermal
effects must be taken into account when sudden changes in the evolution of am-
bient temperature appear.

REFERENCES

1. ELBADRY, M.M., GHALI, A., Temperature Variations in Concrete Bridges. Journal of Structural En-
   gineering ASCE, Vol. 109, No. 10, October 1983.
2. EMERSON, M., The Calculation of the Distribution of Temperature in Bridges. TRRL Report LR561,
   Dept. of the Environment, Transport and Road Research Laboratory. Crowthorne, Berkshire, 1973.
3. HOFFMAN, P.C., McCLURE, R.M., WEST, H.H., The Temperature Problem in a Prestressed Box Girder
   Bridge. The Pennsylvania Transportation Institute, The Pennsylvania State University, University
   Park. January 1984.
4. LEONHARDT, F., KOLBE, G., PETER, J., Temperaturunterschiede gefährden Spannbetonbrücke. Beton
   und Stahlbetonbau, Vol. 60, No. 7, July 1965.
5. MIRAMBELL, E., Criterios de diseño en puentes de hormigón frente a la acción térmica ambiental.
   Tesis doctoral. E.T.S. de Ingenieros de Caminos de la U.P.C. Barcelona, Marzo 1987.
6. MIRAMBELL, E., AGUADO, A., Modelo de obtención de distribuciones de temperaturas y tensiones lon
   gitudinales autoequilibradas en puentes de hormigón. Revista Internacional de Métodos Numéricos
   para Cálculo y Diseño en Ingeniería, Vol. 3, No. 2, Abril 1987.
7. PRIESTLEY, M.J.N., BUCKLE, I.G., Ambient Thermal Response of Concrete Bridges. Road Research
   Unit, Bulletin No. 42, National Roads Board, New Zealand. Wellington, 1979.

Numerical Technique to Simulate Temperature Distributions in Bridges

Méthode numérique d'evaluation des températures dans les ponts

Numerische Methode für die Schätzung der Temperaturfelder in Brücken

Pedro MENDES
Res. Assist.
Techn. Univ. of Lisbon
Lisbon, Portugal

Fernando BRANCO
Assoc. Prof.
Techn. Univ. of Lisbon
Lisbon, Portugal

SUMMARY
A numerical method for the evaluation of the temperature distribution in bridges, based on a finite element solution of the Fourier equation, is presented and illustrated with some examples. Heat exchanges due to convection, thermal and solar radiation are considered. For concrete bridges the construction phases and the associated heat of hydration temperatures are also analysed.

RÉSUMÉ
Une méthode numérique d'evaluation des températures dans les ponts, consistant en une résolution par éléments finis de l'équation de Fourier, est présentée et illustrée avec quelques exemples. Les échanges thermiques associés à la convection et à la radiation solaire et thermique sont considérés. Pour les ponts en béton, les phases de bétonage et la libération de la chaleur d'hydratation sont aussi analysées.

ZUSAMMENFASSUNG
Eine numerische Methode für die Schätzung der Temperaturfelder in Brücken wird dargestellt. Für die Lösung der Fouriersche Gleichung wird die Methode der Finite Elemente benutzt; und einige Beispiele werden gezeigt. Wärmeaustausch sowohl von Konvektion als auch von Ausstrahlung und Sonnenstrahlung wird berücksichtigt. Die Untersuchung der Temperaturen, die während der Bauphase einer Brücke aus der Hydratationswärme des Betons resultieren, wird auch gemacht.

1. INTRODUCTION

The thermal effects on bridges are of major concern to design engineers. The bridge superstructures are subjected to seasonal and daily temperature changes arising from the heat transfers associated with the air temperature and sun radiation.

The seasonal variation corresponds to the maximum mean temperature change that can be expected and its value is usually referred in the design codes. The daily temperature variations are mainly associated with the thermal differentials in the structure and their definition usually needs a special analysis of the bridge characteristics and environment.

These temperature gradients have been the source of several problems mainly associated with excessive displacements during construction (steel structures) or cracking problems during service life (concrete structures).

During the construction of concrete bridges the temperatures due to heat of hydration may also be a source of cracking problems if the thermal gradients lead to tensile stresses exceeding the tensile strength of young concrete.

In this paper a numerical technique to evaluate the temperature differentials in bridges considering the environment interaction and the heat of hydration is presented. The use of this technique is illustrated with the study of the thermal behaviour of composite box girder bridges during construction and of a railway concrete box girder bridge.

2. METHOD OF ANALYSIS

To study the temperature distribution in a bridge a two-dimensional analysis is considered. since temperature is assumed to be constant along the bridge axis. The basic equation of the transient thermal phenomena. which relates the temperature T. in each point of the cross section. to the time t. is:

$$\rho c \, \partial T / \partial t = k \left(\partial^2 T / \partial x^2 + \partial^2 T / \partial y^2 \right) + q_v \tag{1}$$

where k, ρ, c are the thermal conductivity. specific mass and specific heat of the material. respectively. and q_v is the rate of heat generated (by hydration. for example) per unit volume.

The boundary conditions associated with eq. (1) may be expressed as

$$k \left(\partial T / \partial x \cdot n_x + \partial T / \partial y \cdot n_y \right) + q = 0 \tag{2}$$

where n_x, n_y are the direction cosines of the unit outward vector normal to the boundary surfaces and q is the amount of energy transferred between the surface and the environment due to convection. thermal irradiation and solar radiation [1].

In concrete bridges. the total amount of heat Q generated until any instant due to hydration of cement may be computed by [2]

$$Q = B + E \exp (-\alpha \ (t_e)^{-n})$$
(3)

where **B, E, α, n** are constants depending upon the mix proportions of the concrete and the type of cement. obtained from experimental tests under a reference uniform temperature T_r. The variable t_e is an equivalent time of the variable temperature process. obtained by

$$t_e = \sum_{o}^{t} 2^{(T-T_r)/10} \Delta t$$
(4)

where **T** is the temperature of the process. assumed constant during the time interval Δt.

The numerical solution of **eq. (1)** is accomplished considering a finite element analysis in the cross section and integrating with respect to time by the finite difference method [3]. For the study of heat of hydration temperatures sequential construction phases are considered rebuilding the finite element mesh and boundary conditions whenever a new phase begins.

3. CASE STUDIES

3.1 Behaviour of Composite Box Girder Bridges During Construction

In the last few years. composite steel-concrete box girder bridges have been widely used for intermediate span bridges. During construction. the girder is often a flexible open section. which subjected to thermal differentials may present important deformations.

Based on the numerical technique referred above the temperature distribution was determined for an open box girder instrumented during construction. The comparison between experimental and analytical results is shown in **Fig.1**. showing a reasonable agreement **[1,4]**
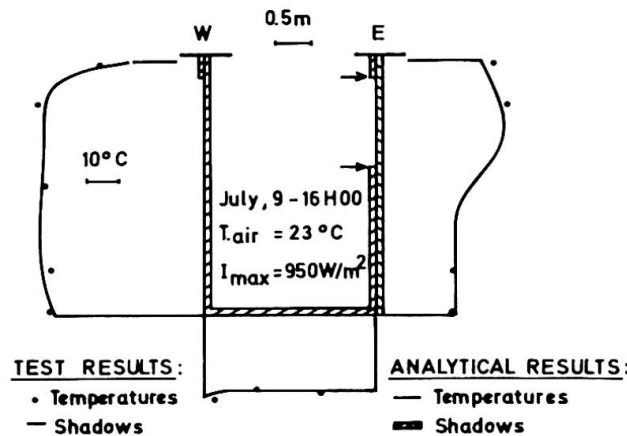
Fig .1 - Comparison between experimental and analytical results [1]

Considering typical geometries a parametric study was then developed to obtain the maximum differentials between the average temperatures of the steel plates. **Fig.2** shows the highest values obtained for summer and winter clear days.

These open box girders under temperature differentials suffer lateral displacements and twist. This behaviour can be studied using a simplified folded-plate analysis where each plate is assumed as a beam and compatibility is imposed at the longitudinal joints [1].

Fig. 2 - Temperatures in an open box girder [1]

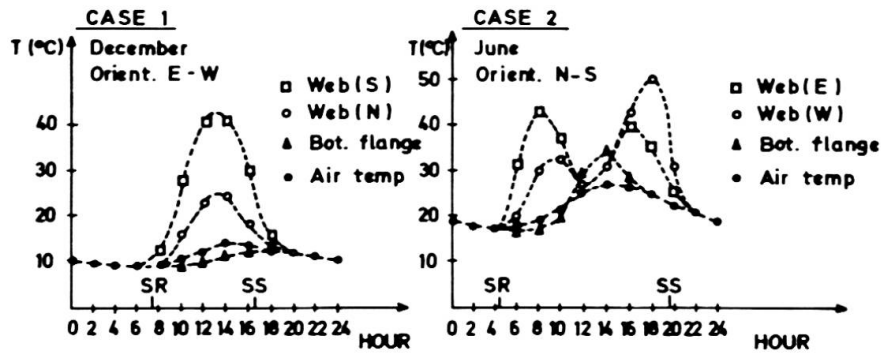Due to the temperature twist ($\emptyset_T$) the self weight (p) becomes an eccentric load with a sinusoidal eccentricity along the span. This effect increases the twist of the girder and the total twist ($\emptyset_{TOT}$) becomes

$$\emptyset_{TOT} = \emptyset_T + \emptyset_p \qquad (5)$$

where $\emptyset_p$ is the increment due to self weight, which can be approximately computed by an non-uniform torsion analysis [1]. In **Fig. 3** the self-weight rotational effect is illustrated for an open box girder.
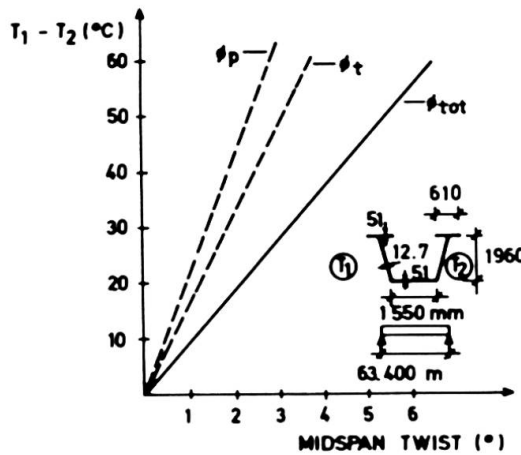
Fig. 3 - Self-weight rotational effect [1]

3.2 Behaviour of a Railway Double Box Girder Bridge

The study of the temperature distributions to be considered in the analysis of a concrete double box railway bridge is now illustrated for the construction and service phases.

3.2.1 Heat of Hydration Effects

The temperatures due to heat of hydration that may arise during the concreting of the superstructure were analysed with the referred numerical technique. First, experimental tests have been made with concrete cubes in order to estimate the concrete hydration properties **(eq. 3)**.

A reasonable   agreement   between analytical and   experimental results was obtained
(Fig. 4) [5]. A construction plan was then assumed for the concreting phases of the deck
and the evolution of the temperatures was determined along the first 10 days **(Fig. 5).**
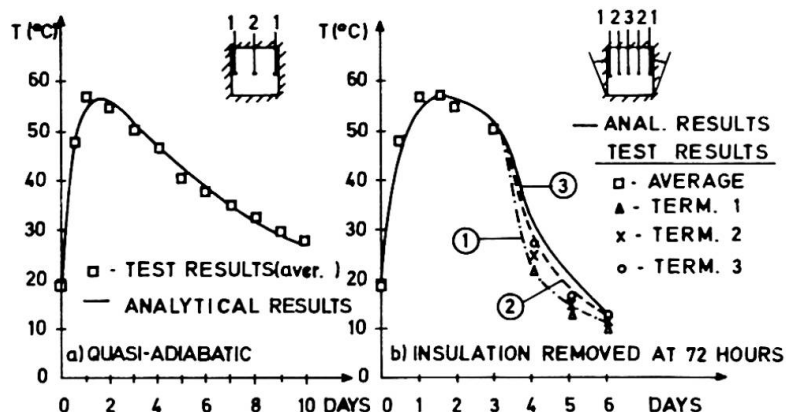
Fig. 4 - Concrete cubes testing
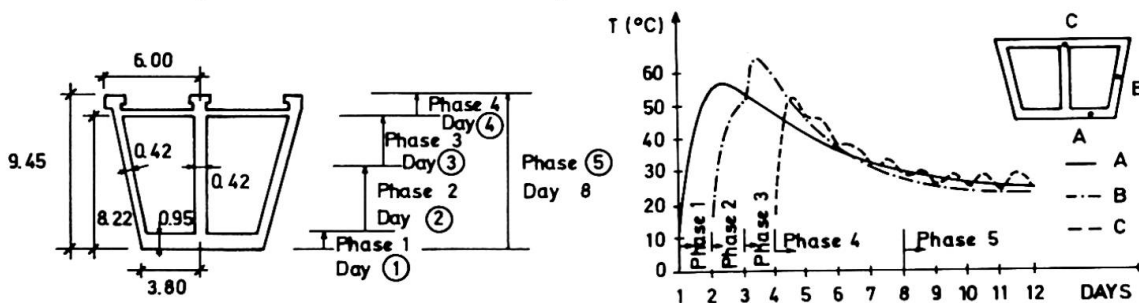
Fig. 5 - Construction plan and temperature evolution in the deck

3.2.2 Deck Temperature Gradients due to Environment Effects

The temperature distribution in each cross-section may be divided into an uniform (mean)
temperature, a linear diagram and an eigen-temperature diagram. The maximum thermal
gradients that are likely to occur in the girder and in the piers under summer conditions are
shown in **Fig.6**, where the influence on vertical gradients of a concrete layer over the deck
for support of the rails can be noticed .
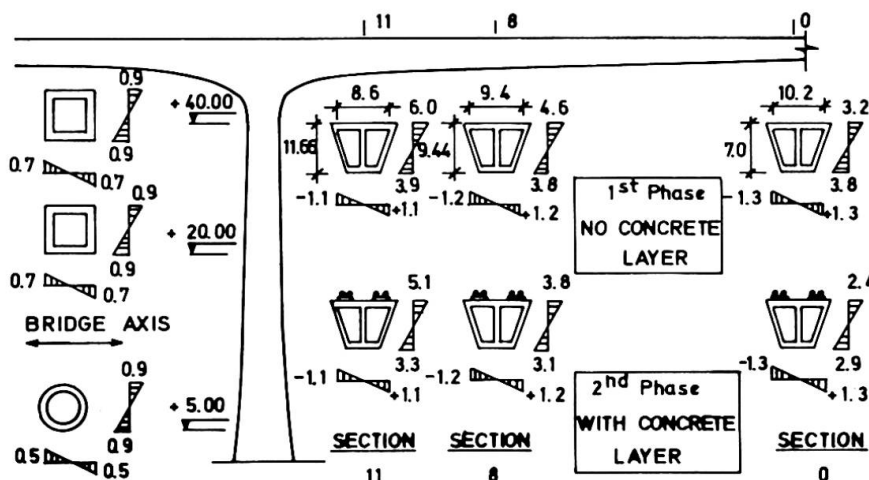
Fig. 6 - Maximum thermal gradients under summer conditions

3.2.3 Rails - Girder Differentials

The use in this bridge of long welded rails and a nonballasted deck imposed the study of the rail-structure interaction due to their temperature differential. The estimation of these differentials was also accomplished with the referred technique. taking into account the environment conditions of the bridge. **Fig. 7** shows the evolution along the day of the mean temperatures of the rail and of the girder, with a maximum value obtained around 3:00 p.m..
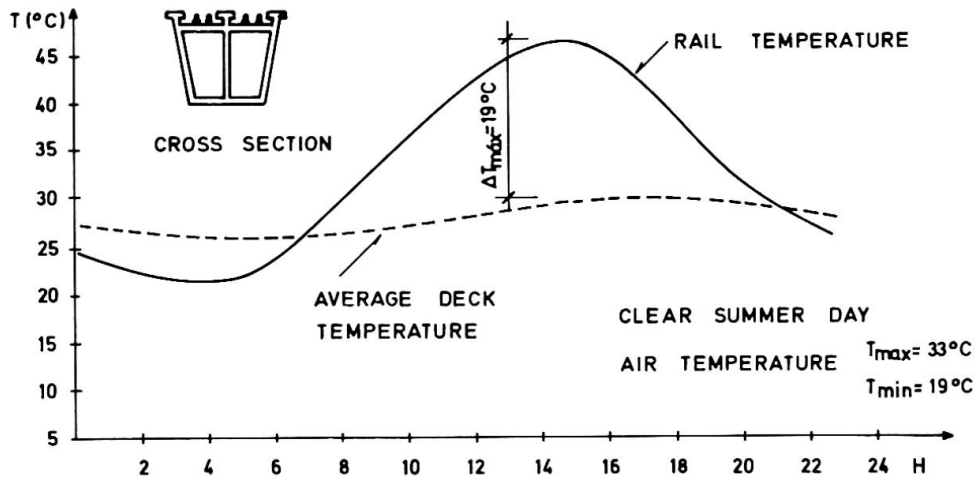
Fig 7. - Mean temperatures in the rails and in the deck

4. CONCLUSIONS

This paper presents a numerical technique to obtain the temperature distribution in bridges due to environment conditions and to cement heat of hydration. The applicability of this technique is illustrated with several examples.

ACKNOWLEDGEMENTS

The work reported herein is part of a continuing research program on thermal effects on bridges developed at CMEST - Technical University of Lisbon.

REFERENCES

1. BRANCO F.A.. Composite Box Girder Bridges - Structural Behaviour during Construction (in Portuguese). Doctoral Thesis, Tec. Univ. of Lisbon. 1984.

2. RASTRUP E.. Heat of Hydration of Concrete. Magazine of Concrete Research, vol. 6 No. 17, 1954.

3. BRANCO F.A., MARTINS L. and MENDES P., Program TEMP - A Numerical Solution of the Heat Transfer Problem. Report CMEST DEC. DT. 21, Lisbon, 1986.

4. BRANCO F.A.. Thermal Effects on Composite Box Girder Bridges during Construction. Second International Conference on Short and Medium Span Bridges, Ottawa, 1986.

5. BRANCO F.A. and MENDES P.. Heat of Hydration Temperatures in Bridges. RILEM 1st International Congress, Paris, 1987.

Thermal Stresses in Concrete Bridges

Contraintes thermiques dans les ponts en béton

Temperaturspannungen in Massivbrücken

Jiři HEJNIC
Chief Engineer
Inst. Traffic and Struct. Eng. Design
Prague, ČSSR

Jiři Hejnic, born 1935, received his civil engineering degree from the Czech Technical University in Prague, Czechoslovakia, in 1958. In 1976 he was awarded a PhD for his work on thermal stresses in concrete bridges. He has designed several large prestressed concrete bridges built in Czechoslovakia.

SUMMARY
Temperature stresses in concrete bridges result from the heat released during cement hydration and from insolation and ambient heating. In the paper thermal properties of concrete are discussed. The main results of thermal analysis and experimental research of temperature distribution on two large prestressed concrete bridges built in Prague, Czechoslovakia in recent years are presented. It is shown that in special cases temperature stresses have even greater magnitude than live load stresses.

RÉSUMÉ
Les contraintes thermiques dans les ponts en béton résultent de la chaleur se produisant au cours de l'hydratation du ciment, de l'insolation et de la chaleur ambiante. Cette étude décrit aussi les qualités thermiques du béton armé et présente les résultats principaux de l'analyse thermique et des recherches expérimentales de la distribution de température de deux ponts en béton précontraint construits à Prague, Tchécoslovaquie, dans les années récentes. L'étude montre aussi que dans des cas spéciaux, les contraintes thermiques ont une variation plus grande que les contraintes causées par les charges du trafic.

ZUSAMMENFASSUNG
Temperaturspannungen in Massivbrücken entstehen bei der Entwicklung der Hydratationswärme sowie infolge Sonnenstrahlung und Umgebungswärme. Der Beitrag umfasst eine Beschreibung der Temperaturstoffkennzahlen für Beton. Die Hauptergebnisse der Berechnung der Temperatur- und Spannungsfelder sowie Temperaturmessungen an zwei grossen Spannbetonsbrücken, die in den letzten Jahren in Prag, Tschechoslowakei, gebaut wurden, werden vorgestellt. Es ist daraus ersichtlich, dass in Spezialfällen die Temperaturspannungen sogar grösser sind als die Spannungen aus Verkehrslasten.

1. INTRODUCTION

For many years concrete bridges have been designed mainly for dead and live load stresses. In-situ measurements carried out in last decades have shown that in special cases stresses of the same or even greater magnitude can be caused by thermal loads, creep and shrinkage. While the effects of creep and shrinkage have been studied for many years and several organisations as CEB or FIP have given international recommendations for calculation of these effects, thermal response of concrete structures is a complex phenomenon nearly ignored in conventional design.

Restraints of free thermal expansions induce stresses. Localised stresses may be caused by the thermal incompability between cement mortar and aggregate which affect concrete durability. In concrete bridge design the main sources of heating are as follows:
- Insolation and ambient heating. Bridges thermally respond to solar radiation, wind exposure, and ambient temperature changes, both daily and annual cycles.
- The heat released during cement hydration. This is more important in relatively thick sections, as bridge abutments, piers and decks.

The major form of heat input is solar radiation. Although the soffit and external web surfaces may receive an amount of reflected radiation from the surroundings, this will generally be a small proportion of the direct radiation on the deck surface. Convective heat transfer occurs at the surface when a temperature difference exists between the surface and the surrounding air, and is accentuated by movement of air along the surface. Radiative losses may occur from the surface to adjacent colder surfaces or to the sky.

The reaction of cement with water is exothermic and releases a considerable quantity of heat. Modern cements are finer, and have increased outputs of heat. The temperature distribution in mass-concrete structures depend on the amount and rate of heat-of-hydration emission, and the three-dimensional heat flow. The former is a function of cement type, mix design and concrete temperature, while the latter is a function of ambient conditions, the properties of concrete, insulation and temperature distributions. The most important temperature differences are these between the hot interior and the colder surface in a few days after concreting.

Over each time increment the incremental thermal stress is the product of the incremental restrained strain and the concrete elastic modulus. The modulus is, however, a function of both time and temperature, with the early strains inducing very little thermal stresses. Thermal stresses in mass structures are significantly affected by creep. So the thermal stress distribution is a complex function of the inter-related parameters of creep, time, elastic modulus and temperature. Cracking alters the stress distribution, and thus, the change in concrete tensile strength with time and temperature should be considered.

2. THERMAL PROPERTIES OF CONCRETE

For the concrete bridge design and specially for the calculation of thermal stresses main thermal properties of concrete, as conductivity, specific heat, thermal diffusivity, thermal expansion coefficient, hydration heat of cement and surface heat transfer coefficient should be known. Many investigations have been made for large concrete dams while there thermal stresses are usually far more significant than live or dead load stresses. Unfortunately, concrete technology for these structures is quite different than that for concrete bridges. Generally, for concrete mix not thermal properties, but high ultimate strength and sufficient workability are most important in bridge technology.

Thermal conductivity measures the ability of the material to conduct heat. The conductivity of concrete depends on its degree of saturation, composition, porosity, density, temperature, and mineralogical character of the aggregate and

ranges generally between about 1.3 and 2.3 $(J.s^{-1}.K^{-1})$. For concrete mix in concrete bridges with high density and low porosity the conductivity reaches the higher value.

Thermal diffusivity represents the rate at which temperature changes within a mass can take place. The range of typical values of diffusivity of concrete is between $5 . 10^{-7}$ and $10 . 10^{-7}$ $(m^2.s^{-1})$. Because of the influence of moisture in the concrete on its thermal properties, diffusivity should be measured on speciments with a moisture content which will exist in the actual structure.

Specific heat, which represents the heat capacity of concrete, is considerably increased by an increase in the moisture content of the concrete. It is little affected by the mineralogical character of the aggregate, and depends also on the actual range of temperature. The common range of values for concrete with a normal moisture content is between 0.84 and 1.20 $(J.g^{-1}.K^{-1})$.

Thermal expansion coefficient of concrete depends both on the composition of the mix and on its hygric state at the time of the temperature change. Thermal expansion coefficient varies between $7.0 . 10^{-6}(K^{-1})$ for limestone – concrete and $13.0 . 10^{-6}(K^{-1})$ for quartzite – concrete.

The heat of hydration is the quantity of heat, in Joules per gram of unhydrated cement, evolved upon complete hydration at a given temperature. The temperature at which hydration takes place greatly affects the rate of heat development. In fact, the heat of hydration depends on the chemical composition of the cement, and the heat of hydration of cement is very nearly a sum of the heat of hydration of the individual compounds when hydrated separately. For usual Portland cements the complete heat of hydration ranges generally between about 300 and 500 $(J.g^{-1})$. For separate compounds the heat of hydration in $(J.g^{-1})$ varies between 500 and 570 for C_3S, 180 and 270 for C_2S, 830 and 910 for C_4A, and 290 and 420 for C_4AF.

Surface heat transfer coefficient is a function of wind speed, concrete temperature, and moisture content. A relation between the top surface heat transfer coefficient h $(J.m^{-2}.s^{-1}.K^{-1})$ and wind speed w $(m.s^{-1})$ can be written as follows: $h = 11.4 + 4.66 w$.

3. TEMPERATURE CHANGES ON THE KLEMENT GOTTWALD BRIDGE

3.1 Measurement programme

The Klement Gottwald Bridge over the Nusle valley in Prague (Fig. 1), built in 1973, is at present the largest prestressed concrete bridge in Czechoslovakia. During the construction of the bridge a large – scale research programme was under way, one item of which consisted in measuring the temperature of concrete in the superstructure. The temperatures were measured in two phases: 1° – during the hydration process of concrete; 2° – after the construction works were finished. In the latter phase the influence of ambient temperature changes and of insolation has been investigated with special regard to the forming of temperature gradients, and the resulting temperature stresses. In the superstructure (Fig. 2) altogether 139 thermocouples were embedded in the concrete, the elements being arranged in five cross-sections. The first phase of measurements took place in December 1969 when very low outside temperature was registered. In the second phase the concrete temperatures were measured in August 1973, when the influence of various outside atmosphere conditions was investigated /1/.

3.2 Measurements during the development of hydration heat

The temperatures of concrete, as they were ascertained in December 1969, have been influenced mainly by the following factors:
- Exceptionally low outside temperature, since during all the time interval when measurings were under way the temperature of air kept steadily below zero (^oC)
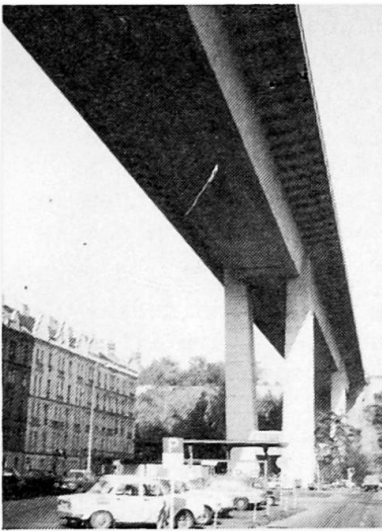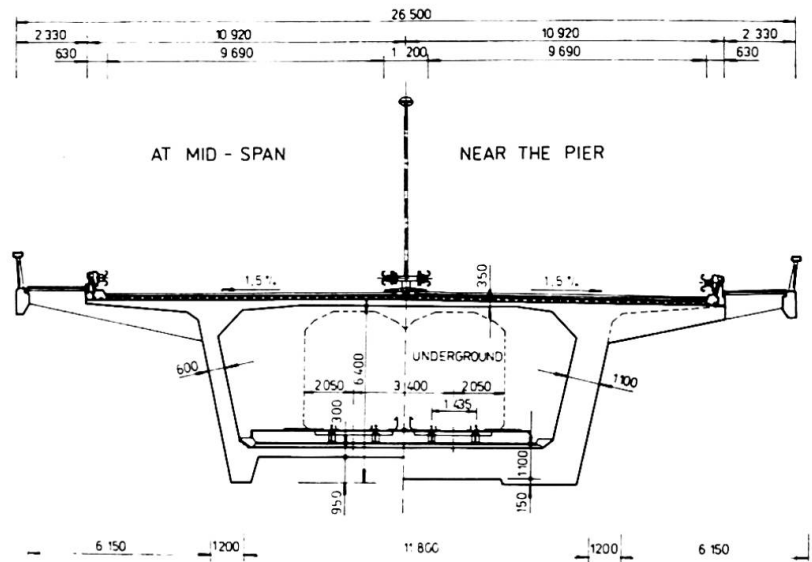
Fig.1 Klement Gottwald Bridge

Fig.2 Cross section of the bridge

as from Fig. 4 can be seen.
- Pre-heating of the concrete mix so that the temperature at placing of the mix
  was some 35°C on the average. Hot air blow was used for protection of placed
  concrete against frost.

The concreting of each lamella 3,5 m in length was carried in 3 phases - the
bottom slab, the walls and at last the top slab with the rigid frame corner and
the cantilevers. In Fig. 3 the distribution of temperature in the cross section
24 hours after placing of concrete in the top slab, i.e. 7 days after the concre-
ting of the walls is shown. At this time-point the temperature in the corner was
51.1°C, while in greater part of the walls and in the whole bottom slab the con-
crete temperature was deep below zero. The time-distribution of temperature in
the upper corner (point a in Fig. 4 - in a thermocouple 0.80 m under the top
surface of the upper slab) is shown in Fig. 4. The highest temperature-reading
56.0°C corresponds to the time point when the heating of concrete by means of
hot air blow was finished.
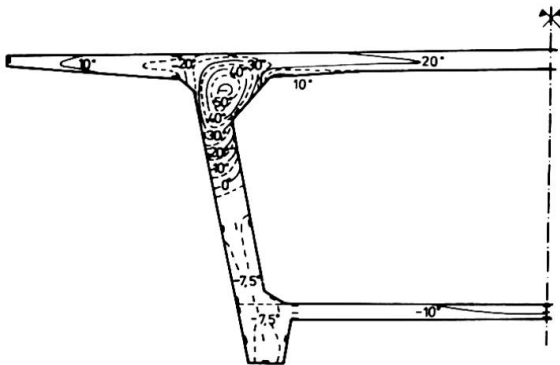
Fig.3 Temperature distribution
in the cross-section
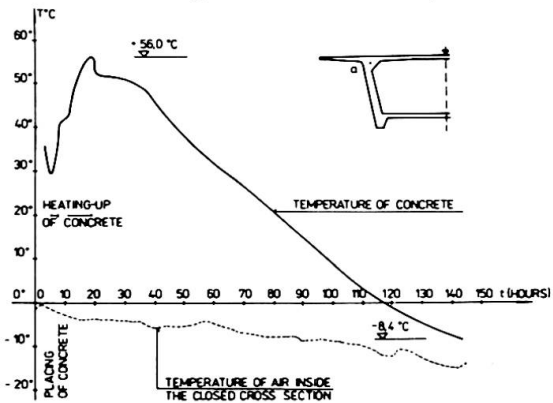
Fig.4 Time-distribution of
temperature in the upper corner a

3.3 Concrete temperatures and stresses due to ambient temperature changes

Temperature of the concrete of the finished superstructure has been measured
with respect to the influence of ambient temperature changes and of insolation,
the measurings being performed in August 1973. The influence of various outside
atmospheric conditions has been investigated, from simple temperature change
without insolation to the influence of very intensive insolation. The wall ex-
posed to insolation changes its temperature rapidly. Since the temperature vari-
ation throughout the concrete is not linear, this gives rise to secondary
compressive stresses near the outer surface.

The temperature gradients in the bridge cross-section, as measured on August 9th, at 6,00 in the morning are shown in Fig. 5. The measurements show that the temperature of the bridge deck is quite stationary due to asphalt insulation and wearing surface, while the temperature gradients in the walls and the bottom slab reach comparatively high values – about 4°C per 30 cm of depth. This part of the bridge is intensively cooled off by cold air flow in the valley. The analysis of thermal stresses using a computer for a finite element method response is based on the measured characteristics of the temperature field. For the iso-thermal lines shown in Fig. 5 the computed stresses can be seen from Fig. 6. Maximum tensile stresses reach 2.04 N.mm^{-2} while the structural analysis gave for the whole live load maximum tensile stress 1.93 N.mm^{-2}.
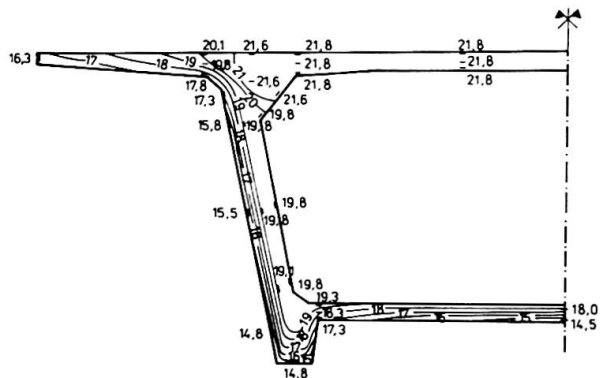
Fig. 5 Temperature field on August 9th in the morning
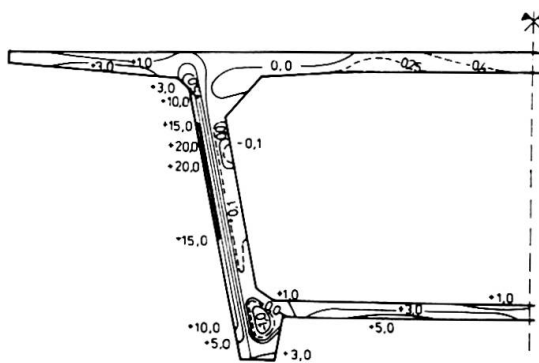
Fig.6 Tensile stresses due to temperature field on Fig. 5

4. ANALYSIS AND MEASUREMENTS OF THERMAL STRESSES ON ANTONÍN ZÁPOTOCKÝ BRIDGE

4.1 Measurements and analysis programme

The Antonín Zápotocký Bridge in Prague (Fig. 7) is the latest large and very irregular structure crossing the river Vltava built in 1988 /2/. During the construction experimental research of strains, stresses and temperature was carried out. The four main piers have prestressed concrete capping beams more than 39 m long, 5 meters high and from 2 to 4.4 meters wide where more than 600 cu.m. of concrete Class 40 was placed in one operation. Since the contractor could not ensure the cooling of the concrete mix or its components, it was necessary to analyse also the state of stress of the structure due to development of hydration heat. Fourier's equation which describes heat movement in the capping beam was solved using triple integral of Jacobi Theta function. Basic assumption for the stress analysis was that the elastic modulus of concrete varies with time in the same manner as the heat-of-hydration emission /3/. Thermal stresses were computed taking concrete creep in consideration. During the construction of the main four piers measurements of hydration heat and strains were carried out to

Fig.7 Antonín Zápotocký Bridge across the Vltava

prove agreement between theoretical temperature and stress distribution and ex-
perimental research.

4.2 Main results of thermal stress analysis and measurements

A general programme of thermal field and stress analysis was prepared for a
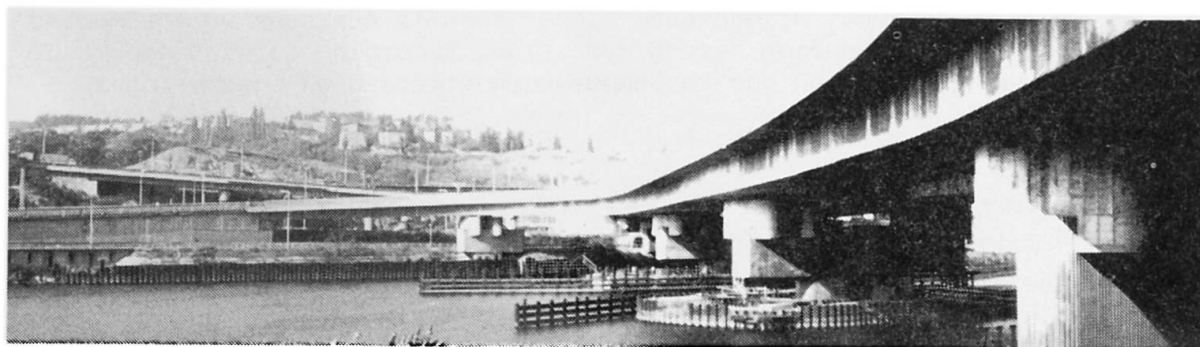9825 T Hewlett Packard calculator according to the complexity of the problem to
be solved, where thermal properties of concrete as discussed in chapter 2 were
applied. From Fig. 8 the main results of thermal field analysis can be seen.
Thermal stresses due to the thermal field are shown in Fig. 9. At the beginning
tensile stresses develop near both surfaces of the capping beam wall, reaching
maximum 3.6 $N.mm^{-2}$ 5 days after concrete placing. One year later these tensile
stresses change in compressive stresses about 0.7 $N.mm^{-2}$ near the concrete sur-
face. Fig. 10 shows the temperature distribution as measured 5 days after comple-
ting the placing of concrete in the capping beam of the pier. The measured strains
showed principal agreement with the values obtained from the calculation.
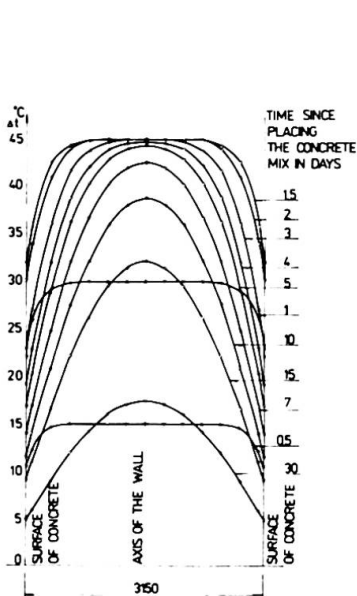
Fig.8 Temperature
distribution in the
capping beam wall
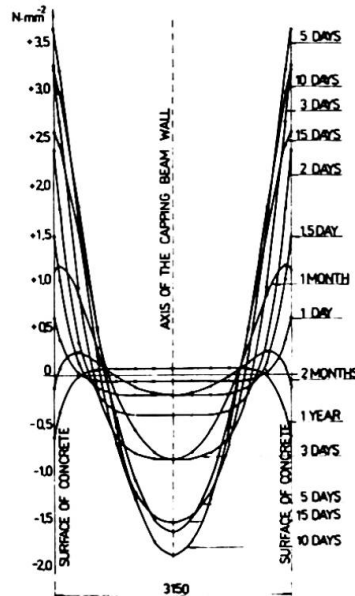
Fig.9 Thermal stresses
due to temperature
distribution in Fig. 8
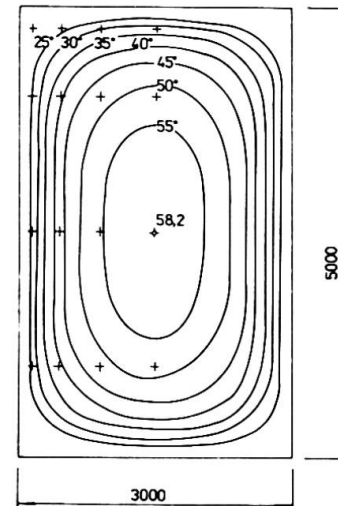
Fig.10 Measured tempera-
ture field 5 days after
placing of concrete mix

5. CONCLUSION

Thermal analysis and experimental research of temperature distribution on two
large bridges in Prague, Czechoslovakia showed interesting results. On the Kle-
ment Gottwald Bridge the tensile stresses due to temperature gradients influenced
by the cold wind in the valley were found higher than those for the whole live
load. On the Antonín Zápotocký Bridge even higher tensile stresses were computed
caused by the heat released during cement hydration. According to high amount of
mild steel no cracking was found due to temperature stresses on both bridges.

REFERENCES

1. HEJNIC J., Effect of Temperature Changes on Prestressed Concrete Bridge,
   7th Congress FIP, New York, 1974.

2. HEJNIC J., New Bridge Across the Vltava in Prague, 12th Congress IABSE,
   Final Report, p. 1021 - 1028, Vancouver, 1984.

3. GIESECKE J., Berechnung von Wärmespannungen in Massenbetonbauwerken bei linear
   veränderlichem Elastizitätsmodul, Der Bauingenieur, Oktober 1968.

Heat Transfer and Thermal Stresses in the Singapore Cable Tunnel

Transfert de chaleur et effets thermiques dans le tunnel immergé à Singapour

Wärmeleitung und thermische Spannungen im Untersee -Kabeltunnel in Singapur

O. P. JENSEN
Civil Engineer
CNT-CONSULT
Copenhagen, Denmark

O. P. Jensen, born 1947, obtained his M.Sc. Degree from the Technical University in Copenhagen. He has specialized in immersed tunnel and off-shore design and participated both in studies and detailed design. O. P. Jensen was in charge of the prestressing and soil-structure modelling for this tunnel.

Davar ABI-ZADEH
Mechanical Engineer
Ove Arup and Partners
London, England
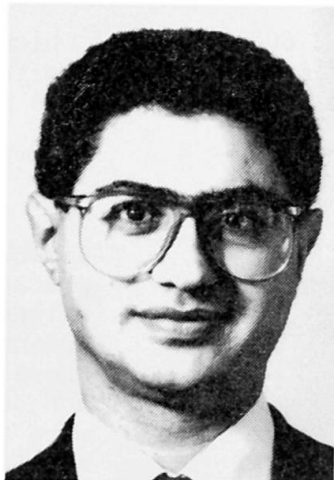
Davar Abi-Zadeh, born 1944, obtained his PH.D. from the Imperial College, University of London for his work in AGR Steam Generators. Since, he has been involved in development of fluid flow and heat transfer models for industrial applications. He is now a consultant, designing mechanical systems in industrial and technological buildings.

SUMMARY

In 1986 a 2.6 km long undersea cable tunnel in Singapore was completed. The heat generated by the power circuits is removed from the tunnel by means of a cooling water system and a ventilation system. Heat transfer calculations were carried out and formed the basis for the structural stress analysis.

RÉSUMÉ

En 1986, la construction d'un tunnel immergé de 2,6 km de longueur a été achevée à Singapour. La chaleur produite par les câbles haute – tension a été éliminée du tunnel du moyen d'une installation de refroidissement par eau et d'un système de système d'aération. Les calculs de ce transfert de chaleur ont formé la base de l'analyse des contraintes dans le tunnel.

ZUSAMMENFASSUNG

Im Jahre 1986 wurde der 2,6 km lange Untersee-Kabeltunnel in Singapur fertiggestellt. Die Abwärme aus dem Transport elektrischer Energie wird mittels eines Kühlwassersystems und einer Lüftungsanlage aus dem Tunnel entfernt. Wärmeleitungsberechnungen bildeten die Grundlage der Spannungsanalysen für den Tunnel.

1. INTRODUCTION

In April 1985, the Public Utilities Board of Singapore (PUB) awarded to Christiani & Nielsen A/S a contract for the design and construction of an immersed cable tunnel from Pulau Seraya across the Jurong Strait to Mainland Singapore.
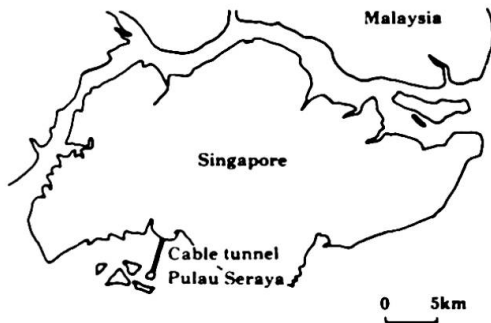
Fig, 1 Tunnel Location

At the time of award, a 1750 MW power station was under construction on Pulau Seraya. This station has now been commissioned, supplying electrical power to Singapore since January 1987.

The construction of the immersed tunnel, two terminal buildings, mechanical and electrical installations was completed by the end of 1986.

The contract was awarded as a result of international tendering based on an outline design and specifications prepared by Mott, Hay & Anderson Asia Pte. The detailed design of the immersed tunnel and the planning of the construction methods were done by Christiani & Nielsen while Ove Arup and Partners, London were engaged for the design of the terminal buildings, the mechanical/electrical installations and ancillary services in the tunnel.

2. THE SUBMERGED CABLE TUNNEL

The immersed cable tunnel is 2,600 m long of which 1,800 m has a floor level 23 metres or more below main sea level. The tunnel consist of 26 nos. 100 metres long elements with overall dimensions of 6.50 m wide x 3.70 m high.
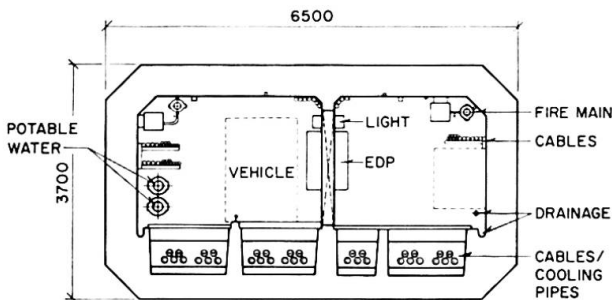
Fig. 2 Cross-section of cable tunnel

The 100 metres long tunnel elements were made up of 29 precast segments. These were aligned and prestressed longitudinally on a marine lift where 80% of the mechanical and electrical installations were also fitted. After launching from the marine lift, each element was towed into position, sunk, founded and backfilled.

3. COOLING SYSTEMS

3.1 Cable Loading and Troughs

The maximum normal cable loading is established as being a total of continuous load of the power station at 2000 MVA and 230 kV. There are seven cable circuits each designed for 500 MVA.

The power circuits and associated cooling pipes are arranged in flat formation in troughs which are back-filled by a lean mix concrete of 0.8 W/m°K thermal conductivity. The west bore, Figure 3, houses four circuits

which generate 365 W/m heat at full load. The east bore houses two troughs, one containing a single circuit with heat generation of 89 W/m and the other containing two circuits with heat generation of 181 W/m when operating at full load. Any number of the seven circuits can be loaded in any combination at full or part load subject to the maximum total continuous load.

3.2 Water Cooling System

Each power circuit is associated with two piped cooling water circuits, each pipe designed for a flow rate of 3 kg/s at maximum outlet temperature of 40°C. The cooling water is pumped from Pulau Seraya Terminal cooling towers to the tunnel cable through pipework to extract heat from power circuits. The heated water is then discharged at the Pandan Road Terminal cooling towers. The water is cooled and pumped back to the cable troughs in the tunnel. The cycle is continuously repeated. The cooling equipment is provided with 100% standby and situated at the two terminals. Equipment at each terminal is designed for 50% of the total cooling requirements.

Power circuits generate heat which is primarily removed by cooling water. The rate of heat removal, q, as advised by the cable contractor depends on the loading of cables. The maximum values are 52, 121 and 261 W/m for a single circuit, two circuits in one trough and four circuits in the same bore respectively. The excess heat which cannot be removed by the cooling water system dissipates by ventilating air and by transmission to the tunnel structure, sea and seabed.

3.3 Tunnel Ventilation

The tunnel ventilation system provides environmental control of the tunnel atmosphere whilst unmanned, during maintenance occupation and in an emergency.

Six axial flow, vertical mounted, two speed, two stage, contra rotating, reversible fans are located in the Pulau Seraya terminal building. The fans operate in two banks, one bank per bore. Each bank is operated in various fan, stage and speed combinations to suit the three conditions. There are three modes of fan operatin for each bore.

i)   A single fan operates continuously at low speed with one stage working to achieve the minimum air velocity of 1 m/s required for heat dissipation, whilst maintaining a tunnel air temperature not exceeding 40°C. Ambient air at maximum temperature of 33°C is drawn into each bore via the Pandan Road terminal building. It is then passed via segregated shafts into the respective bores. The fans extract the vitiated air from the tunnel and exhaust it to atmosphere at the Seraya terminal building.

ii) Two fans operate at low speed with both stages working to achieve the minimum tunnel air velocity of 2.5 m/s, required for ventilation with the tunnel occupied and all services in operation and with maximum normal operating condition at the power circuits.

iii) The fans are capable of being manually set in the high speed and reverse modes from the fireman's control panels situated at either end of the tunnel for smoke removal. The fans either extract smoke from the tunnel in the normal direction or are reversed to draw in air and exhaust instead through the Pandan Road terminal. Two fans operate at high speed with both stages working to achieve tunnel air velocities of 5 M/s in the normal mode or 4.5 m/s in the reverse mode.

4.0   THE HEAT TRANSFER MODEL

4.1   Objective and Assumptions

The heat transfer model is developed to check that the ventilation system corresponding to the different modes of operation will maintain a tunnel air temperature of less than 40°C when any combination of power circuits are under maximum normal load, and to investigate the temperatures that will result along the tunnel at various surfaces of the tunnel cross section.

The steady state heat balance equations for air and two cable cores in the west and east bores have been solved to arrive at air temperature distribution along the tunnel. Assumptions have been made that, (i) the heat conduction and convection coefficients are constant along the tunnel, (ii) axial and peripheral conduction is negligible, (iii) at any cross section, the air temperature in each bore and temperature of each cable core are constant.
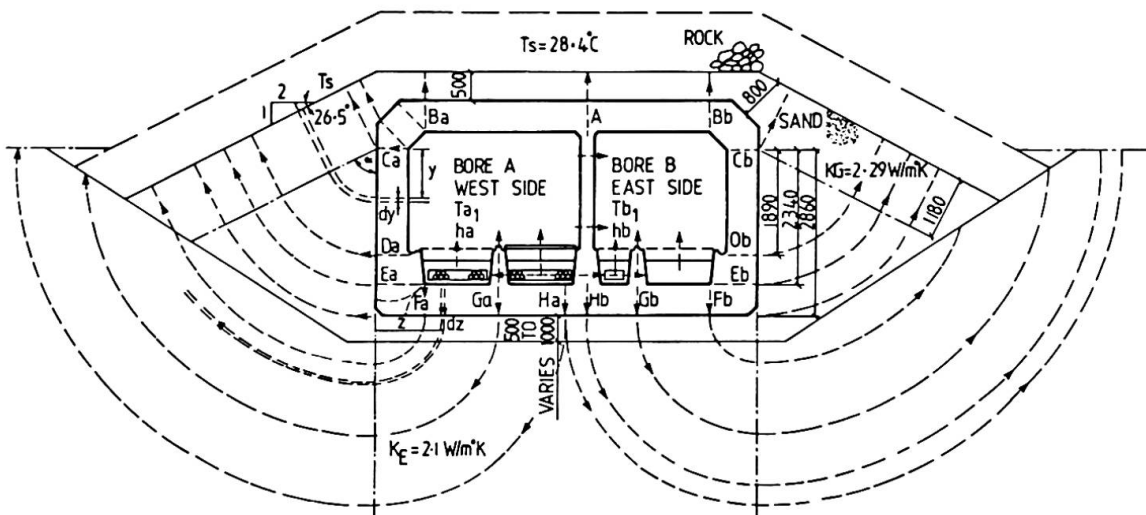
Fig. 3 Heat Conduction Model

4.2   The Heat Conduction Model

Figure 3 shows the heat conduction model at a cross section of the tunnel. The perimeter of the tunnel has been divided into a number of section, as AB, BC, CD, etc. on Figure 3, for which a set of uniform heat-flow path is designated. In mapping the path, attention has been given to experimental studies in [1] and [2], and it is assumed that the internal and external concrete surfaces for each section are isotherms. The paths in each section have then been used for calculating the heat conductance (W/°K) per unit length of the tunnel.

The conductances of appropriate sections have been added to find the total conductances corresponding to the heat transfer between cable cores, air and sea.

4.3   Energy Balance Equations

Referring to Figure 3, the heat balance equations for air, Cable Core 1 (Outer trough) and Cable Core 2 (Inner trough) at a discrete length ΔL, m, along the tunnel are:

Bore A

$$(MC)_a \frac{\Delta T_a}{\Delta L} + K_{a1}(T_a-T_s)+K_{ab1}(T_a - T_b)=K_{a21} (T_{ca1} - T_a)+K_{a22} (T_{ca2}-T_a) \quad (1)$$

$$K_{a21} (T_{ca1} - T_a) + K_{a31} (T_{ca1} - T_s) + K_{a4} (T_{ca1} - T_{ca2}) = q_{a1} \quad (2)$$

$$K_{a22} (T_{ca2}-T_a)+K_{a32} (T_{ca2}-T_s)+K_{a4} (T_{ca2}-T_{ca1})+K_{ab2}(T_{ca2}-T_{cb2})=q_{a2} \quad (3)$$

Bore B

$$(MC)_b \frac{\Delta T_b}{\Delta L}+K_{b1} (T_b-T_s)+K_{ab1} (T_b-T_a)=k_{b21} (T_{cb1}-T_b)+K_{b22} (T_{cb2}-T_b) \quad (4)$$

$$K_{b21} (T_{cb1} - T_b) + K_{b31} (T_{cb1} - T_s) + K_{b4} (T_{cb1} - T_{cb2}) = q_{b1} \quad (5)$$

$$K_{b22} (T_{cb2} - T_b)+K_{b32}(T_{cb2}-T_s)+K_{b4} (T_{cb2}-T_{cb1})+K_{ab2} (T_{cb2}-T_{ca2})=q_{b2} \quad (6)$$

Where M and C are mass flow rate and specific heat of air and T is tempe-rature. Subscripts a, b and c refer to bore A, bore B and cable core re-spectively. Conductance, K(W/m) is defined as follows:

K_1 Air and Sea, K_{21} Air and Cable Core 1 (the outer trough), K_{22} Air and Cable Core 2 (the inner trough) and sea, K_4 The Two Adjacent Cable Cores in each bore, K_{ab1} Air in Two Bores, K_{ab2} The two Adjacent Cable Cores in Two bores. Heat transfer coefficient inside the tunnel has been calculated from:

$$Nu = 0.023 \, Pr^{.3} \, Re^{.8},$$ Where, $Re = (VD/\nu)$, $Nu = (hD/k)$, and Pr is the Prandtl number. At each discrete interval, it is assumed that:

$$\Delta T_a = (T_{a2} - T_{a1})/2, \quad \Delta T_b = (T_{b2} - T_{b1})/2, \quad T_a = (T_{a2} + T_{a1})/2,$$
$$T_b = (T_{b2} + T_{b1})/2$$

Where (T_{a1}, T_{b1}) and (T_{a2}, T_{b2}) denote the air temperatures at inlet and outlet of a discrete length respectively. Boundary conditions at the tun-nel ends are:

$$T_{a1} = T_{b1} = T_{ambient}$$ at x = 0 and T < 40°C at x = 2600 m

T_a, T_b, T_a and T_b are substituted into equations 1 to 6 and the resulting equations have been solved for the unknown parameters T_{a2}, T_{b2}, T_{ca1}, T_{ca2}, T_{cb1} and T_{cb2} at each intervals. Computation has been carried out on a micro computer for different modes of operation and cable loading.

The model provides the average temperatures that will result along the tunnel at various surfaces of the tunnel cross section together with the air and cable core temperature.

The analysis indicates that the surface of the inner trough in he west bore can reach to a maximum temperature of 64°C at the "unmanned" mode of operation when three power circuits in the west bore (two circuits in the inner trough) and one single circuits in the inner trough of the east bore are loaded at 2000 MVA.

The model does not account for the effect of moisture evaporation from the tunnel walls. Therefore, the results obtained for dry air are conservative in regard to the amounts of heat transferred between the air and the tun-nel, as the effect of evaporation is to decrease the temperatures of air and tunnel surfaces from those predicted for dry air conditions.

A separate model for periodic analysis based on the modified method in [3] indicates that the variation of maximum temperature due to changes in the ambient temperature would be minor.

5.0   STRESS-ANALYSIS

In the longitudinal direction the bending moments and shear forces were calculated by use of a soil-structure interaction model and from this the number of tendons were determined.

The stress calculation results fulfil the stress requirement for normal operation condition with minimum compression stress 2 Mpa and extreme operation condition with minimum stress 0.0 Mpa. The number of tendons were governed by the two conditions, both conditions included temperature loads.

After sinking, the element is backfilled and locked with an initial axial compression force due to the water pressure. The heat generation from the power circuits will increase the temperature inside the tunnel and thereby cause an increase in the axial compression force already built into the tunnel element.

The non-uniform temperature increase over the cross section due to the position of the circuits at the bottom of the tunnel, following maximum gradients and temperature differences was achieved from the heat transfer calculations

- Gradient roof $2.5^{\circ}C$
- Gradient bottom $1.0^{\circ}C$
- Temperature different roof and bottom $10.9^{\circ}C$

The gradients and the temperature different cause a tension stress in the roof of 2.2 Mpa which was taken into account during the determination of the number of the tendons.

ACKNOWLEDGEMENT

REFERENCES

1.   BILLINGTON N.S., Heat Loss Through Solid Ground Floors, JIHVE, November 1951

2.   ASHRAE, Handbook of Fundamentals, Chapter 25, 1986

3.   PEAVY B.A., Heating and Cooling of Air Flowing Through an Underground Tunnel, C. Engineering and Instrumentation, J. of Research of the National Bureau of Standards, Vol. 656, No. 3, July 1961

Wasserundurchlässiger Beton – Rissbildung und Feuchtigkeitstransport

Watertight Concrete – Cracking and Moisture Transport

Béton impermeable – fisuraton et transport d'humidité

Mario FRIEDMANN
Dr.-Ing.
Betontechnologisches Institut
Berlin

Mario Friedmann, geb. 1954, promovierte als Bauingenieur an der Technischen Universität Berlin. Nach seinem Studium und Ingenieurbautätigkeit in Chile ist er nach Deutschland übersiedelt; dort ist er seit 1979 gutachterlich tätig. Nach einer 2-jährigen Tätigkeit in der Industrie ist er Mitinhaber eines Institutes geworden; er ist mit Gutachten, Diagnose, Ausschreibung und Bauleitung von Bauschäden und Instandsetzungsmaßnahmen befaßt.

ZUSAMMENFASSUNG

Bei Bauwerken aus wasserundurchlässigem Beton wird eine weitgehende Rissefreiheit des Betonbauteils gefordert, so daß Risse weder infolge von Lasteinwirkungen noch infolge der aus der Hydratation des Zementes freiwerdenden Wärme und den daraus resultierenden Spannungen entstehen dürfen. Weiterhin ist zu berücksichtigen, daß wasserundurchlässiger Beton nicht wasserdicht ist: d.h., daß die in geringer Menge durch das Bauteil transportierte Feuchtigkeit von der dem Wasser abgewandten Seite des Bauteils wieder verdunsten können muß. Ist die Austrocknung durch dampfdichte Schichten (z.B. einen PVC-Fußbodenbelag) behindert, so können infolge der langsamen Wasseransammlung Bauschäden entstehen. Zur Erfassung der Eigen- und Zwängungsspannungen, sowie zur Ermittlung der durch das Bauteil transportierten Wassermenge, werden praxisgerechte Bemessungsverfahren angegeben.

SUMMARY

Structures built of watertight concrete require that they remain substantially free of cracks that may arise not only in consequence of loads but also due to the stresses resulting from the heat released in the hydration process of cement. It must furthermore be considered that what is commonly referred to as watertight concrete is not in fact completely impermeable to water: actually, the small amounts of moisture that are transported through the concrete must be able to evaporate on the face not in contact with the water. If such drying is prevented by a vapour barrier (e.g. a PVC-floor covering) damage may develop in consequence of the gradual accumulation of water. The internally induced and restraint stresses and the determination of the water amount transported through the concrete are described.

RÉSUMÉ

Les éléments de bâtiments construits en béton imperméable requièrent une absence quasi complète de fissures qui se formeraient non seulement sous l'influence de charges mais qui seraient aussi le résultat de tensions dues à la chaleur dégagée lors de l'hydratation du ciment. Il faut en outre tenir compte du fait que le béton imperméable n'est pas étanche: les petites quantités d'humidité transportées à travers le béton doivent pouvoir s'évaporer à la surface qui n'est pas en contacte avec l'eau. Si un tel séchage est empêché par une barrière à vapeur (p.ex.un revètement du sol en PVC), des dommages dûs à l'accumulation graduelle de l'eau pourraient en découler. Des procédés de calcul pour les tensions internes et résiduelles et pour déterminer la quantité d'eau transportée à travers le béton sont donnés.

1. DEFINITION UND BAUSTOFF

Unter einem wasserundurchlässigen Beton wird ein Beton verstanden, durch den Wasser so langsam transportiert wird, daß die durch das Bauteil durchgedrungene Wassermenge auf der dem Wasser abgewandten Seite wieder verdunsten kann. Im Gegendazu wird unter einem wasserdichten Beton ein Beton verstanden, in den das Wasser weder eindringen noch durchzudringen vermag.

Da durch den wasserundurchlässigen Beton in sehr begrenztem Umfang Wasser durchtreten kann, ist die Anwendung wasserundurchlässiger Betone als wasserdruckhaltende Dichtung zu vermeiden bei

- elektrischen Betriebsräumen

- dynamisch erregten Bauteilen (Rißgefahr),

- lagerräumen, die zur Aufbewahrung feuchtigkeitsempfindlicher Güter dienen (z.B. Papierlager o.ä.

- Bauteilen mit einer wasserdichten Oberfläche auf der dem Wasser abgewandten Seite (z.B. bei Sohlen mit wasserdichtem PVC-Fußbodenbelag) und bei

- Vorhandensein von aggressivem Grundwasser.
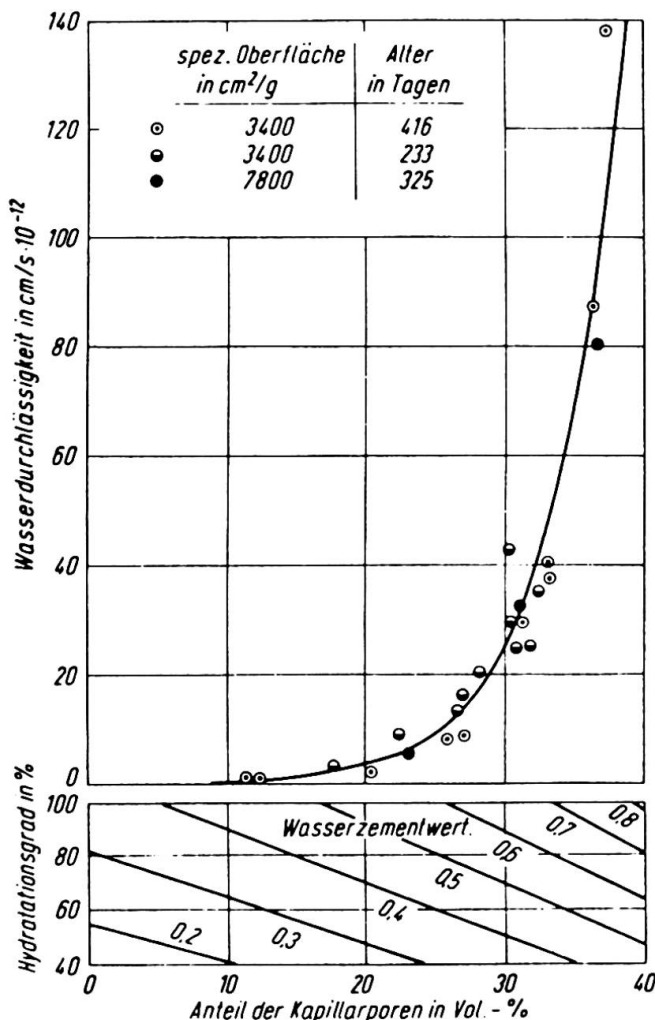
Bild 1. Wasserdurchlässigkeit von Zementstein in Abhängigkeit von Kapillarporosität und Wasserzementwert [1]

Beton ist von Natur aus ein poröser Baustoff, der aus einer Mischung von Zuschlägen (ca.70%), Bindemitteln und Wasser besteht. Die Wasserdurchlässigkeit des Betons wird im wesentlichen von der Dichtigkeit des Zementsteines beeinflußt, wenn man unterstellt, daß die Zuschläge in der Regel wasserdicht sind. Je geringer der Wasserzementwert des Betons ist, um so höher ist seine Dichtigkeit, da weniger Überschußwasser im Beton vorhanden ist, das bei Verdunsten die für den Wassertransport maßgeblichen Kapillarporen im Zementstein hinterläßt. Die Verringerung der Kapillarporen und damit die Erhöhung der Wasserundurchlässigkeit ist durch folgende Maßnahmen erreichbar:

1. Zusammensetzung des Betons nach einer stetigen Sieblinie, sowie Verdichtung und Nachbehandlung des Betons (feucht halten), so daß ein hoher Hydratationsgrad schneller erreicht werden kann (Bild 1).

2. Reduzierung des Wasserzementwertes (Bild 1).

3. Einsatz von Betondichtungsmitteln im Zusammenwirken mit den Maßnahmen nach 1 und 2.

Entsprechend den Untersuchungen in [1] wirken Betondichtungsmittel bei Vorhandensein von drückendem Wasser nicht immer verbessernd oder haben eine nur unbedeutende Wirksamkeit. Nach heutiger Erkenntnis wird deswegen die Was-

serundurchlässigkeit des Betons im wesentlichen durch die geeignete Zusammensetzung des Betons und dessen gute Nachbehandlung auch ohne Betondichtungsmittel erreicht.

2. PROBLEM DER RISSBILDUNG INFOLGE HYDRATATIONSWÄRME

2.1 Übersicht

Für ein wasserundurchlässiges Bauwerk ist notwendig, daß der Beton frei von durchgehenden Rissen bleibt. Risse im Beton entstehen im wesentlichen durch ungleichmäßiges und behindertes Schwinden, Setzen, äußere Lasten und Temperaturspannungen. Deswegen ist es erforderlich, daß das statische System übersichtlich ist und zwangsauslösende Verbindungen vermieden werden.

2.2 Hydratationsbedingte Temperaturen

Die bei der Hydratation des Zementes freiwerdende Wärme verursacht einen Temperaturanstieg im Bauteil. Dieser Temperaturanstieg hängt im wesentlichen von folgenden Parametern ab:

- dem Betonalter,
- der Bauteildicke,
- der Zementart,
- der Zementmenge (mindestens 350 kg/m^3 für einen wasserundurchlässigen Beton) und
- der Art der Nachbehandlung des Betons (Wärmedämmung, Betoninnenkühlung, Dauer der Feuchtlagerung).

In Bild 2 wird der Einfluß des Betonalters, der Bauteildicke und der Zementart auf dem Temperaturanstieg im Bauteilkern gezeigt: Es ist ersichtlich, daß mit zunehmender Bauteildicke, die freiwerdende Wärme langsamer abgeführt wird (im Extremfall liegt der adiabatische Fall für d→∞ vor), so daß dann der Temperaturanstieg im Betonkern am größten wird. Die Bauteilfläche (Länge und Breite) hat nahezu keinen Einfluß auf die entstehenden Temperaturen.

Die Größe der Spannungen im Betonquerschnitt ist direkt dem Temperaturgradienten zwischen den Plattenrändern und dem Kern proportional. Der Temperaturgradient zwischen Kern und Plat-
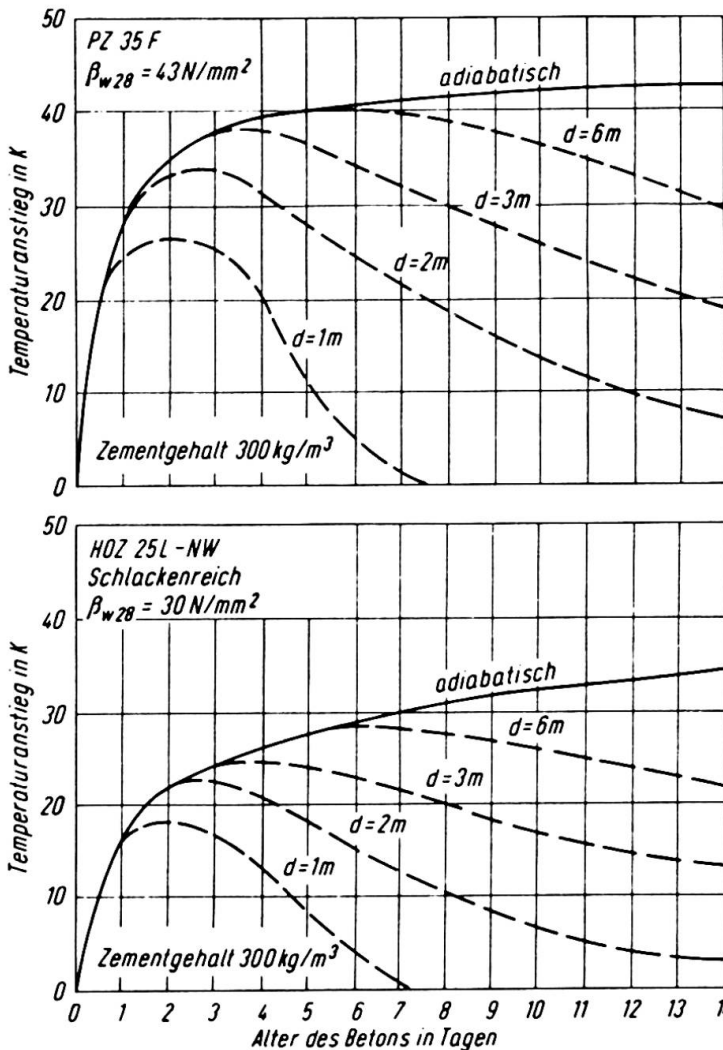
Bild 2. Verlauf des Temperaturanstieges im Kern von Bauteilen unterschiedlicher Dicke d [2]

tenoberseite läßt sich wirkungsvoll durch eine auf der Fundamentplatte angeordnete Wärmedämmung verringern. In Bild 3 ist die Temperaturdifferenz zwischen Kern und Betonoberfläche in Abhängigkeit von der Zeit für eine Platte ohne und mit wärmedämmender Abdeckung angegeben:
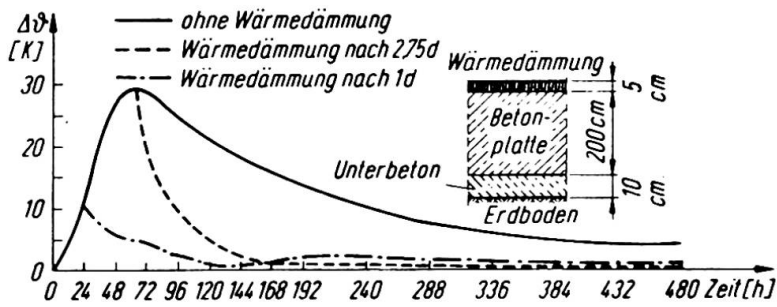
Bild 3. Temperaturdifferenz zwischen Kern und Plattenoberfläche in Abhängigkeit von der Zeit für oberseitig gedämmte Platten nach t=1d, t=2,75d und t= ∞ (ohne Wärmedämmung)

Bild 4. Temperaturgefälle über die Plattendicke (200 cm)

ε_s mittlere Dehnung

$\Delta\varepsilon_s$ Krümmung

Bild 5. Eigenspannungen in einem Betonquerschnitt

Wenn Wärmedämmung 24h nach dem Betonieren verlegt wird, sinkt die max. Temperaturdifferenz zwischen Kern und Oberfläche von 30°C (ohne Wärmedämmung) auf 10°C.

Die Temperaturdifferenz kann noch stärker verringert werden, wenn die Wärmedämmung zeitlich früher verlegt wird ($\Delta\vartheta$= 8°C bei Verlegung der Dämmung 9 h nach dem Betonieren).

2.3 Hydratationsbedingte Spannungen

2.3.1 Übersicht

Wie im Abschnitt 3.2 dargestellt, wird beim Erstarren und Erhärten des Betons Wärme frei, die zu einem Temperaturanstieg im Beton führt. In Bild 4 ist die Temperatur über dem Plattenquerschnitt in Abhängigkeit von der Zeit für eine 2 m dicke Fundamentplatte dargestellt: Es ist ersichtlich, daß in den Randbereichen eine deutliche Temperaturabsenkung bezogen auf das Platteninnere auftritt, weil dort ein Wärmeaustausch mit der umgebenden Außenluft bzw. dem Erdreich stattfindet. Im Innern der Fundamentplatte, wo die entstehende Wärmemenge nicht so schnell abgeführt wird, kommt es damit zwangsläufig zu einer Temperaturerhöhhung. Aufgrund des im Querschnitt veränderlichen Temperaturgradienten $(\vartheta_m - \vartheta_a)$ bzw. $(\vartheta_i - \vartheta_m)$ (s.Bild 5)sowie aufgrund des ungleichförmigen Schwindens $\Delta\Delta\varepsilon_s$(s.Bild 5) stellt sich im Betonquerschnitt ein Eigenspannungszustand ein. Wenn die Längenänderung des Bauteils infolge des Temperaturanstiegs ϑ_m (s.Bild 5)oder der mittleren Schwinddehnung durch Reibung oder durch eine kraftschlüssige Verbindung mit einem anderen Bauteil verhindert wird, entstehen Zwängungsspannungen. Der Nachweis der Eigen- und Zwängungsspannungen kann anhand der in [3] enthaltenen Angaben geführt werden.

4. FEUCHTETRANSPORT DURCH BAUTEILE AUS WASSERUNDURCHLÄSSIGEM BETON

Die Problematik der Wassertransportvorgänge in porösen Baustoffen ist noch nicht eindeutig geklärt. In [4] sind Rechenprogramme entwickelt worden, um - unter gewissen Randbedingungen -

die Transportvorgänge rechnerisch zu erfassen. Für baupraktische Konstruktions-
aufgaben kann bei Bauteilen aus wasserundurchlässigem Beton der zu beobachtende
Gesamtfeuchtetransport (makroskopische Feuchtigkeit) näherungsweise nach [4] wie
folgt ermittelt werden:

$$Q = \frac{1}{d} \cdot (FC \cdot \Delta c + FT \cdot \Delta\vartheta + FP \cdot \Delta h) \quad (\frac{g}{m^2 \, d}) \quad (1)$$

Es bedeuten:

FC   Hygrischer Feuchteleitkoeffizient, der von der Theorie der kapillaren
     Flüssigkeitsbewegung in porösen Stoffen ausgeht.

     FC Beton = $10^{-6} (m^2/h) \, \hat{=} \, 24$ (g/md) [4]

     Wassergehaltsdifferenz in den Bauteiloberflächen in m^3 Wasser
     pro m^3 Material

     c ≈ 22 (VOL.-%) gesättigter Beton

     c ≈ 5 (Vol.-%) Beton in der Ausgleichsfeuchte

FT   Thermischer Feuchteleitkoeffizient, der von einem temperaturbedingten
     Feuchtetransport in flüssigem und in dampfförmigem Zustand unter Berück-
     sichtigung von Sorptionsvorgängen ausgeht und primär vom Feuchtegehalt
     des Baustoffes abhängt.

     $10^{-10} \frac{m2}{hk} \leqslant FT \leqslant 10^{-8} \frac{m2}{hK}$ [4]

     Für eine überschlägliche Berechnung des Gesamtfeuchtetransportes kann
     FT wie folgt angenommen werden:

     $FT = 10^{-8} \quad (\frac{m2}{hK}) \, \hat{=} \, 0,24 \quad (\frac{g}{mdK})$

     bei temperaturbedingten Feuchtigkeitsanreicherungen

     $FT = 10^{-10} \quad (\frac{m2}{hK}) \approx 0$ (g/mdK)

     bei temperaturbedingten Austrocknungen

$\Delta\vartheta$ Temperaturdifferenz der Bauteiloberflächen (°K)

FP   Gesamtdruckbezogener Feuchteleitkoeffizient, der die Transportintensität
     durch ein poröses Material infolge eines Gesamtdruckgradienten beschreibt.
     Auch wenn ein "kompakter" Wassertransport durch die Poren eines wasserun-
     durchlässigen Betons nicht stattfinden wird, kann näherungsweise von der
     materialspezifischen Durchlässigkeit nach dem Gesetz von Darcy ausgegangen
     werden [4]:

     $FP \approx 10^{-10}$ (cm/s) $\hat{=}$ 0,1 $(\frac{g}{m \, d})$ (Bild 1)

Δh Gesamtdruckunterschied (m Wassersäule)

d   Bauteildicke (m)

Anhand von Gl. (10) kann die durch einen Bauteil aus wasserundurchlässigem Beton
transportierte Feuchtigkeitsmenge größenordnungsmäßig ermittelt werden. Diese
Feuchtigkeitsmenge muß von der inneren Bauteiloberfläche an die Luft wieder ab-
gegeben werden können (Verdunstungsvorgang). Die Feuchtigkeit Q_v, die von der
Luft aufgenommen werden kann, folgt zu:

$$Q_v = n \cdot m_s \cdot \frac{(100 - \varphi)}{100} \cdot V \cdot 24 \quad (g/m^2 d) \quad (2)$$

Es bedeuten:

Q_v von der Luft aufnehmbare Feuchtigkeitsmenge $(g/m^2 d)$

n   Luftwechselzahl (1/h)

     n = 0,2 bei üblichen Kellerfenstern. Keller wird nichtbelüftet.

     n = 0,5 für Wohnräume

m_s max. Wassergehalt der Luft (g/m^3) (Bild 6)

φ relative Feuchtigkeit (%)

V Auf die Außenwandfläche bezogenes Raumvolumen (m^3/m^2)

Zusammenfassend ist festzustellen, daß der Nachweis einer hinreichenden Feuchtebilanz erfüllt ist, wenn gilt:

$$Q_V \geqq 1,5 \cdot Q$$

Hierbei wird vorausgesetzt, daß die Abgabe der durch das Bauteil transportierten Feuchtigkeit an die Raumluft nicht durch eine dampfdichte Schicht - wie z.B. einem PVC-Fußbodenbelag - behindert wird. Bei Bauteilen aus wasserundurch- lässigem Beton ist konstruktiv sicherzustellen, daß die - wenn auch in geringen Mengen - trans- portierte Feuchtigkeit an die das Bauteil umgebende Luft abgegeben werden kann.
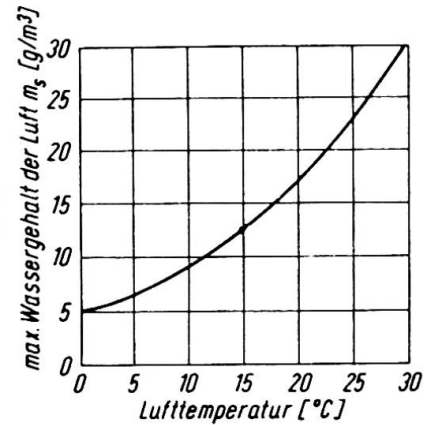
Bild 6. Sättigungsgehalt der Luft an Wasserdampf in Abhän- gigkeit von der Temperatur

5.AUSFÜHRUNGSTECHNISCHE UND KONSTRUKTIVE MASSNAHMEN

Bei der Bemessung und konstruktiven Durchbildung von Bauteilen aus wasserundurch- lässigem Beton wird die Beachtung folgender Empfehlungen nahegelegt:

- Die Mindestdicke der Bauteile aus wasserundurchlässigem Beton soll 20 cm betra- gen. Die Betondruckzone soll mindestens 15 cm betragen.

- Die Betonüberdeckung soll minimal c = 2,5 cm, besser c = 3,0 cm für Beton B 25 betragen.

  Beim Betonieren ist darauf zu achten, daß die Fallhöhe aus dem Trichter gerin- ger als 10-20 cm ist, um Entmischungsvorgängen entgegenzuwirken. Bei weicher Betonkonsistenz (K 3) sollte das Größtkorn einen Durchmesser von 8 mm nicht überschreiten.

- Durch eine Nachverdichtung des Betons bis zu einem Betonalter von ca. 1,5 bis 4 Stunden kann die Wasserdurchlässigkeit und die Rißsicherheit bedingt verbes- sert werden.

- Die Austrocknungsmöglichkeit an der dem Druckwasser abgewandten Seite eines Bauteils muß stets gegeben sein, so daß das durchdringende Wasser wieder aus- trocknen kann.

- Mauerwerksinnenwände, die auf einer wasserundurchlässigen Betonsohle lagern, müssen eine horizontale Abdichtung (kapillarbrechende Schicht) erhalten.

LITERATUR:

1. WITSCHERS, G., und KRUMM, E.: Zur Wirksamkeit von Betondichtungsmitteln.Beton- technische Berichte 1975. Düsseldorf: Beton Verlag GmbH.
2. BASALLA, A.: Wärmeentwicklung im Beton. Zement Taschenbuch 1964/65. Wiesbaden, Berlin: Bauverlag GmbH.
3. CZIESIELSKI, E., und FRIEDMANN, M.: Gründungsbauwerke aus wasserundurchlässi- gem Beton. Bautechnik (1984), H. 9, S. 113-123.
4. KIEßL, K., und GERTIS, K.: Feuchtetransport in Baustoffen. Eine Literaturaus- wertung zur rechnerischen Erfassung hygrischer Transportphänomene. Forschungs- berichte aus dem Fachbereich Bauwesen der Universität Essen - Gesamthoch- schule, Heft 13, 1980.

Bond Properties between Concrete and Ceramic Tiles

Propriétés d'adhérence entre le béton et les carreaux de céramique

Haftfähigkeit zwischen Beton und Klinkerplatten

Dick KARLSSON
Civil Engineer
Partek Corp.
Pargas, Finland
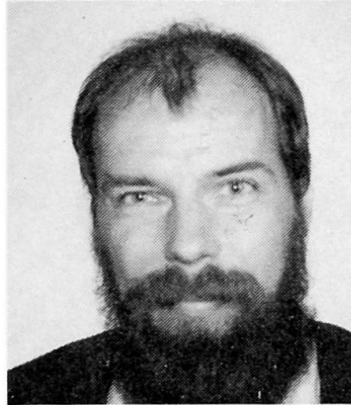
Dick Karlsson, born 1952, received his civil engineering degree at the Helsinki University of Technology. For three years he was involved in developing CAD-programs for Partek's element industry. Now for five years he has been working at Partek's Development Centre in the field of building physics.

SUMMARY

This article deals with the factors affecting the bond between ceramic tiles and concrete in sandwich facade panels. The temperature distribution in a wall has been calculated, and based on this the shear stresses between tiles and concrete. The bond properties of ceramic tiles designed with different texture have been tested in the laboratory by different test methods.

RÉSUMÉ

Cet article présente les facteurs influençant l'adhérence entre des carreaux de céramique et le béton dans des éléments de façade sandwich. La distribution de température dans une paroi est calculée, et s'appuyant sur ces résultats la résistance au cisaillement entre les carreaux et le béton est calculée. Des essais des propriétés d'adhérence des carreaux de céramique avec diverses structures des sont effectuées en labratoire à l'aide de plusieurs méthodes.

ZUSAMMENFASSUNG

Dieser Artikel behandelt die Faktoren, die die Haftung zwischen Klinkerplatten und Beton in Fassadenelementen von Sandwich-Konstruktion beeinflussen. Die Temperaturverteilung in einer Wand ist berechnet worden, und daraus die Schubspannung zwischen Platten und Beton. Die Haftfähigkeitseigenschaften der Klinkerplatten mit verschiedener Oberflächenstruktur sind im Labor mit Hilfe verschiedener Prüfverfahren geprüft worden.

1. INTRODUCTION

The use of concrete sandwich panels, on which ceramic tiles are applied to form the front face, has greatly increased in Finland during the last few years, and the trend is expected to continue in the future, too.

As the panel consists of two materials with different properties, the bond and the interaction between the materials must fulfil certain requirements due to great stresses in the boundary layer.

2. FACTORS INFLUENCING THE BOND STRESSES BETWEEN CONCRETE AND TILES

2.1 Stresses during production

In Finland these elements are generally manufactured by placing the ceramic tiles on the bottom of the mould and concrete is cast directly on the tiles. The concrete is then thermally treated up to a temperature of 50°C to allow the mould to be removed at an age of one day.

In the layer between tiles and concrete stresses will now occur as a result of the following factors:

-        the shrinkage of concrete,
-        different heat contraction in the materials when the panels are cooling,
-        stresses caused by the panels' dead weight during storage and transportation.

Simultaneously with these time-dependent stresses in the boundary layer, the bond capacity between tiles and concrete and the shear strength capacity of the concrete continue to increase during the curing process. It is to be assumed that the time-dependent stress development will in principle follow the curves in Figure 1. In the long run concrete creep is expected to reduce these stresses [1].
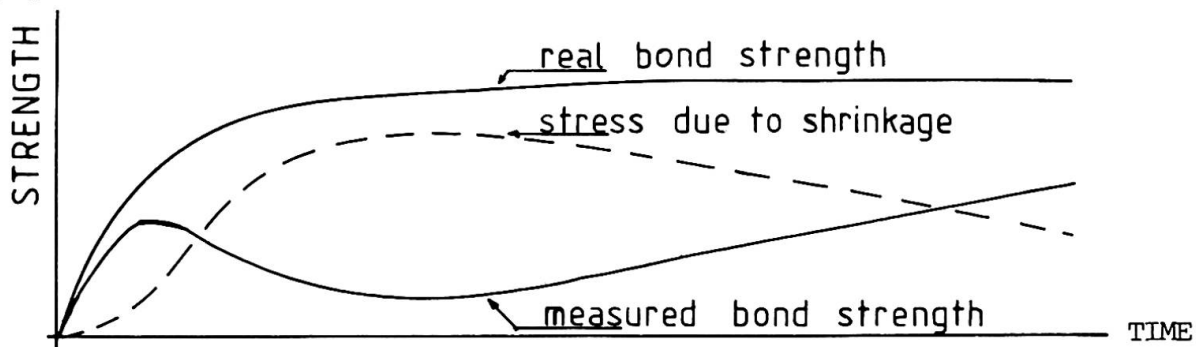

Fig. 1 The development of stresses and strength in the boundary layer between tiles and concrete.

2.2 Stresses caused by climatic actions

These stresses are caused by [2]

-        seasonal differences in temperature,
-        temperature differences related to day and night,
-        variations in humidity,
-        frost-thaw cycles,
-        wind and other mechanical forces.

In this case we can also assume that those stresses related to
seasonal differences in temperature will at least partly be
reduced by the creep of concrete. In the present situation the
influence of frost-thaw cycles would be very slight, because
frost-resistant concrete is generally used.

The crucial and decisive factor is probably the temperature
difference between day and night. It is important to remember
that this relates to the microclimate, and the surface tempera-
ture may show great variations due to solar radiation in daytime
and counter radiation at night.

2.3 Factors influencing the bond capacity between concrete and tiles

To improve the interaction between the tiles and the concrete
attempts could be made to reduce the stresses by changing the
material properties or to strengthen the bond between the tiles
and concrete.

Stresses caused by temperature variations can be reduced by
modifying the concrete composition in order to reduce the coeffi-
cient of thermal expansion and get it close to that of the tiles.
The aggregate is of crucial importance in this respect [3].

Stresses related to the shrinkage of concrete can also be reduced
by a modification of the concrete composition and by suitable
after-curing [4].

In this study emphasis is laid on the role of the surface struct-
ure of the tiles. The results of the study are presented below.

2.4 Analytical solution of the temperature distribution [5]

The temperature distribution in the construction shown i Fig. 2
has been calculated according to Fourier's differential equation
by the aid of a two-dimensional program using the finite element
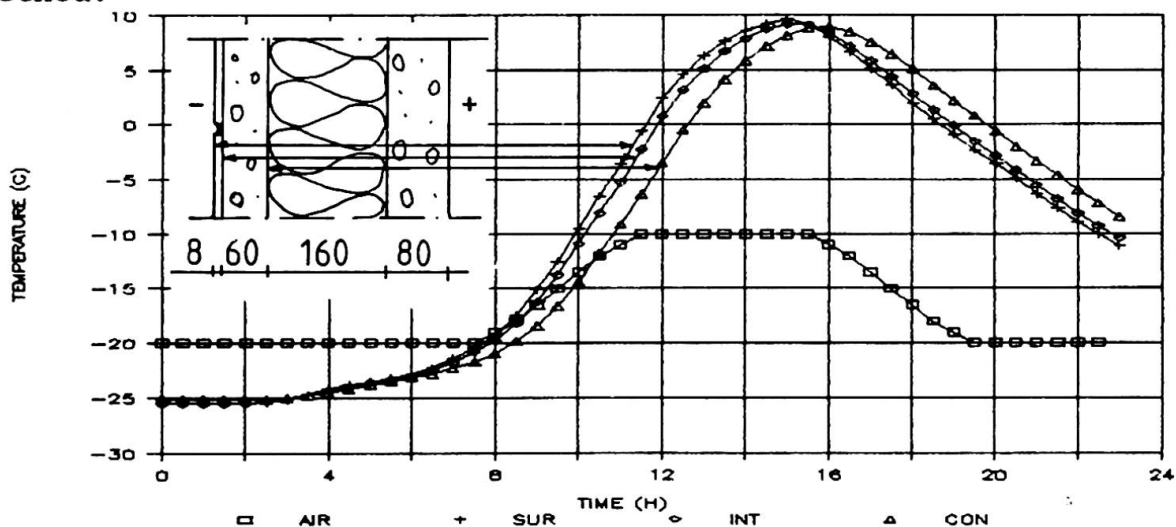method.

Fig. 2 Example of the temperature distribution in the outer
layer of a sandwich element clad with clinker finish;
in mid March in Helsinki.

The figure shows that temperature variations up to 35-40°C during
a day are possible. Field measurements verify these calculations.

3. ANALYTICAL SOLUTION OF SHEAR STRESSES [3]

The tensions between the tiles and the concrete, caused by temperature variations and the different coefficients of thermal expansion, can be calculated according to the equations:

$$\sigma_t = \varepsilon \cdot E_c \cdot A_c \cdot \left(\frac{1}{A_e} - \frac{y_c}{I_e} \cdot y_t \right) \; ; \qquad \tau = \frac{\sigma_t \cdot A_t}{1}$$

where σ_t = compressive stress in tiles (MPa)
         ε = deformation of concrete related to tiles
         E_c = the coefficient of elasticity of concrete (MPa)
         A_c = cross section of the concrete (m^2/m)
         y_c = distance of the centre-of-gravity axis of the concrete to that of the whole cross section (m)
         y_t = distance of the centre-of-gravity axis of the tiles to that of the whole cross section (m)
         τ = shear stresses between tile and concrete (MPa)
         1 = bond length (m)
         A_t = cross section of ceramic tiles (m^2/m)

A_e and I_e are calculated according to the following equations:

$$A_e = A_t + A_c \cdot \frac{E_c}{E_t} \; ; \quad I_e = I_t + y_t^2 \cdot A_t + (I_c + y_c^2 \cdot A_c) \cdot \frac{E_c}{E_t}$$

where E_t = the coefficient of elasticity of tiles (MPa)
         I_t = the moment of inertia of tiles (m^4/m)
         I_c = the moment of inertia of concrete (m^4/m)

With the material properties (E_t = 50,000 MPa, E_c = 25,000 MPa, α_t = 6 x 10^{-6} °C^{-1}, α_c = 10 x 10^{-6} °C^{-1} T > 0°C, α_c = 13 x 10^{-6} °C^{-1} T < 0°C) we can calculate the stresses in the element in Fig. 2 and the following results are obtained:

   ε = 0.23 o/oo, σ_t = - 5.0 MPa, τ = 0.8 MPa

The shear stress   between ceramic tiles and concrete is calculated for an edge tile assuming that the bond length is 50 mm.

4. INVESTIGATION OF THE BOND PROPERTIES OF DIFFERENT TILES

Small concrete elements of 65 x 600 x 1200 mm in size were made to test the influence of the tile bottom structure on the bond. The concrete used was a normal facade concrete with a 28-day compressive strength of K_{28} = 30 MPa. The elements were normally cast with the ceramic tiles on the bottom of the mould and without a jointing compound. They were then stored in conditions where T = 20°C and RH = 95%. The tiles used are specified in Table 1.

Type	Bottom structure	Size [mm]
1	Smooth	8 x 100 x 200
2	Honeycomb, deep profile	8 x 100 x 200
3	Honeycomb, mean profile	8 x 150 x 150
4	Honeycomb, low profile	8 x 150 x 150

Table 1 The ceramic tiles used.

The bond strength of the tiles was determined by drilling a cylinder (ø 78 mm) through the tile about 10 mm into the concrete. An anchor tie beam was fixed to the tile and the tensile strength was determined by a pull-out-method.

The bond was determined at an age of 28 days after the elements had been stored in conditions mentioned above. The bond was also determined according to a Finnish standard, i.e. the frost-thaw test [6], where the element are exposed to 100 frost-thaw cycles between -20 and +20°C. The thawing takes place in water and one cycle lasts 8 hours. Elements only stored in water during the test period are used as reference test specimens.

Moreover, a thermal shock test was used where the elements were placed in a freezer at a temperature of -25°C and the surface temperature of the tiles was raised by IR radiation according to Fig. 3. In this test the length of a cycle was also 8 hours and the number of cycles 100. Then the bond strength was determined. The obtained test results are summarized in Table 2.
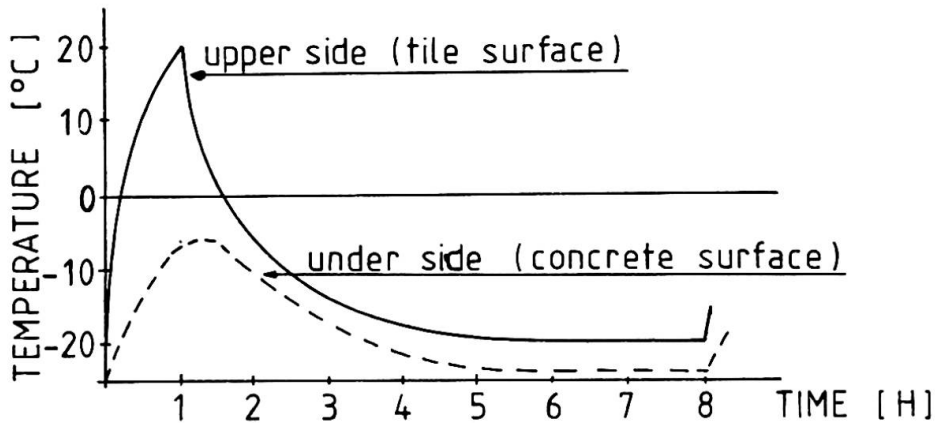
Fig. 3 The rise of temperature in the thermal shock test.

Bond strength (MPa)	Ceramic tiles			
	1	2	3	4
28-day	1.30	1.22	0.84	0.96
Frost-thaw test	0.86	1.12	1.01	0.96
Reference	1.57	1.57	1.53	1.16
Thermal shock test	0 (1)	1.13		
Type of rupture	A	C	B	A

(1)   got loose during drilling.
A =   bond rupture, no concrete on the tile
B =   partial bond rupture, concrete on the tile < 40%
C =   rupture in the concrete surface layer, the tile is covered by a thin concrete layer.

Table 2 Summary of the test results

5. CONCLUSIONS

If attention is only paid to the bond strengths no great differences are observed between the ceramic tiles. The reasons for this are as follows:

- great deviation,
- the bond strength is approaching the tensile strength of concrete,
- the stresses initiated by concrete shrinkage need not to be as great in the different tiles (see chapter 2, Fig. 1),
- the test method is unreliable and not suitable for this test in all respects.

A better conception of the bond is obtained if one looks at the fracture pattern. In this respect tile No.2 and 3 differ clearly from the others.

In my opinion the test method should be changed in order to determine the shear strength in the boundary layer between tiles and concrete instead of the tensile strength.

The thermal shock test also seems to correlate better with the real situation than the frost-thaw test.

The difficulty encountered during all these tests is that the stresses initiated by concrete shrinkage during storage and testing are not known.

Element factories are in a great need for a simple test method for determining the bond capacity. Efforts are made by the Technical Research Centre to develop the desired method.

REFERENCES

1. JOKELA J., HUOVINEN S., Behavior and Design of Concrete Structures under Thermal Gradients. Technical Research Centre of Finland. Research report 338. Espoo 1985. (In Finnish)

2. SJÖSTRÖM C. (ed), HENRIKSSON J. (ed), The Influence of External Environment on Facade Surfaces. The National Swedish Institute for Building Research. Meddelande/Bulletin M:16. Gävle 1987. (In Swedish).

3. ORANTIE K., Facade Elements Clad with Clinker Finish. Technical Research Centre of Finland. Research Report 477. Espoo 1987. (In Finnish).

4. ENCKELL P., Ceramic Mosaic Tiles Used for Exterior Facings on Concrete Wall Panels. Nordisk Betong 1970:2, pp. 131-144. (In Swedish)

5. HEMMILÄ K., Non-stationary Temperature Distribution in Composite Constructions. M.Sc. work. Helsinki University of Technology. Espoo 1981. (In Finnish)

6. Betoniteknillisiä koetusohjeita, osa III. Technical Research Centre of Finland. Research note 3. Espoo 1970.

Wärmedämmung von Kragplatten

Thermal Insulation of Cantilevered Slabs

Isolation thermique des dalles de balcon en porte-à-faux

Daniel BRÜHWILER
dipl. Phys. ETH
EMPA, Abt. Bauphysik
Dübendorf, Schweiz

Daniel Brühwiler, geboren 1961, 1981–86 Physikstudium an der ETH Zürich. Seit 1986 ist er an der Abt. Bauphysik der EMPA tätig und beschäftigt sich mit rechnerischen Problemen der Bauphysik.

ZUSAMMENFASSUNG
In der Massivbauweise sind Wärmebrücken durch tragende Bauteile ein bekanntes Problem. Um dieses bei auskragenden Balkonplatten zu lösen sind seit einiger Zeit Kragplattenanschlussarmierungen mit integrierter Wärmedämmung auf dem Markt. In dieser Arbeit wird auf folgende Frage eingegangen: Welchen Einfluss hat die Variation der Wärmeleitfähigkeit (der Armierung und der Wärmedämmung) auf das Verhalten der Wärmebrücke. Es wird auf Temperaturen und Wärmeverluste eingegangen. Als Werkzeug diente ein Computerprogramm zur Berechnung dreidimensionaler Wärmeströme und Temperaturfelder.

SUMMARY
Thermal bridges in load bearing building elements are a well-known problem in massive construction. To solve this problem relative to cantilevered balconies a system of connecting reinforcement with a thermal break has become available. The following question will be treated in this report: how does variation of the conductivity (of the reinforcement and the thermal break) affect the conditions around the thermal bridge. Temperature and heat flow are considered. A computer program to calculate three dimensional heat flows and temperature fields was used for this work.

RÉSUMÉ
Les ponts thermiques dûs aux éléments porteurs constituent un problème bien connu dans les bâtiments réalisés en construction massive. Afin de résoudre ce problème pour les dalles de balcon en porte-à-faux, on trouve depuis quelques temps sur le marché des armatures de raccordement avec isolation thermique incorporée. Le présent travail étudie l'influence de la variation de la conductibilité thermique (de l'armature et de l'isolation thermique) sur le comportement des ponts thermiques. Les températures ainsi que les déperditions calorifiques ont été considérées. Un programme d'ordinateur permettant de calculer des flux thermiques et des champs de températures tridimensionnels a été utilisé pour ce travail.

1. EINFUEHRUNG

Um den Wärmeschutz bei Kragplatten zu verbessern sind seit einiger Zeit mehrere Produkte auf dem Markt. Es handelt sich dabei um Anschlussarmierungen mit integriertem wärmedämmendem Element (im Folgenden kurz Dämmelement genannt). Die erhältlichen Produkte unterscheiden sich sowohl im verwendeten Stahl als auch im Wärmedämmstoff. Es scheint jedoch einige Unklarheit zu herrschen, welchen Einfluss die verschiedenen Materialien auf den Wärmeschutz ausüben. Die Hersteller beschränken sich meist auf die Bemerkung, dass mit ihrem Produkt eine Verbesserung gegenüber der sonst üblichen Methode des Durchbetonierens erreicht wird. Dies ist verständlich, denn sie müssen den Fragen der Statik, des Korrosionsschutzes und des Brandschutzes erste Priorität beimessen. Es ist nun Ziel dieses Berichtes, die Frage des Wärmeschutzes bei Kragplatten etwas genauer zu beleuchten. Mit Hilfe eines Computerprogramms werden die Temperaturen und Wärmeströme im Bereich eines Kragplattenanschlusses berechnet. Dabei werden unter bestimmten Randbedingungen die Wärmeleitfähigkeiten der Anschlussarmierung bzw. des Dämmelementes variiert.

2. GRUNDLAGEN FUER DIE BERECHNUNGEN

2.1 Standardisierte Anschlussarmierung

In diesem Bericht sollen nicht Produkte sondern Materialien verglichen werden. Deshalb wurde eine standardisierte Anschlussarmierung gemäss Fig. 1 entworfen, die in wärmetechnischer Hinsicht möglichst nahe bei den auf dem Markte angebotenen Produkten steht.

Aus rechentechnischen Gründen ergeben sich zwei Besonderheiten: zum einen ist dies die ungewöhnliche Form der Schubbewehrung, zum andern weist die Armierung einen quadratischen Querschnitt auf. Die Querschnittsfläche entspricht einem Durchmesser von 14mm bei der Zug- und Druckarmierung bzw. 8mm bei der Schubbewehrung.
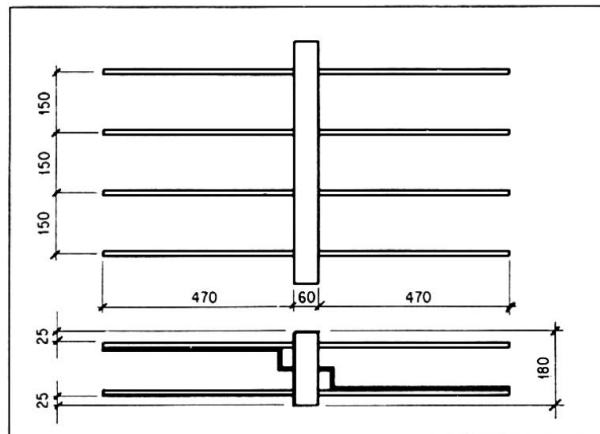
Fig. 1: standardisierte Anschlussarmierung
Alle Masse in mm

2.2 Die Konstruktion

Für die Berechnungen wurde eine Balkonplatte angenommen, die aus einem Zweischalenmauerwerk mit 10cm Wärmedämmung auskragt (Fig.2). Die Ueberdeckung der Armierung beträgt 25mm. Die Decken- bzw. Plattenarmierung geht nicht explizit in die Berechnung ein. Ihr Einfluss sollte durch die Wärmeleitfähigkeit $\lambda = 1.8$ W/mK von Beton berücksichtigt werden. Die Materialien mit ihren Wärmeleitfähigkeiten und die Längenmasse der Konstruktion können Fig. 2 entnommen werden. Die in den Berechnungen variierten Leitfähigkeiten (des Stahls und des Dämmelementes) sind in Tab. 1 enthal-

Fall Nr.	Wärmeleitfähigkeit [W/mK]	
	Stahl	Dämmelement
1	60	0.024
2	60	0.04
3	60	0.15
4	60	0.50
5	15	0.024
6	15	0.04
7	15	0.15
8	15	0.50
9	60	1.8

Tab. 1: variierte Wärmeleitfähigkeiten

ten. Das Dämmelement mit λ=1.8 W/mK entspricht der durchbetonierten Kragplatte. Für Armierungsstahl ist λ=60 W/mK, für Edelstahl 15 W/mK.

Material	Wärmeleitfähig-keit [W/mK]
Backstein	0.44
Beton	1.80
Wärmedämmung	0.04
Trittschall-isolation	0.04
Unterlagsboden	1.50
Dämmelement	variabel
Stahl	variabel
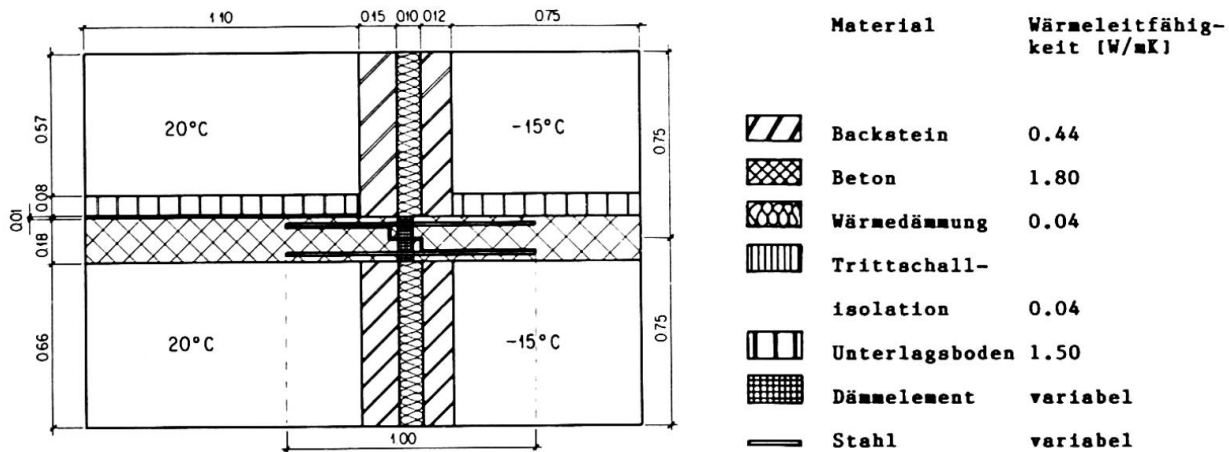
Fig. 2: Zur Beschreibung der Konstruktion. Alle Längenmasse in m.

2.3 Thermische Randbedingungen

Wie aus Fig. 2 ersichtlich beträgt die Lufttemperatur warmseitig +20°C, kaltseitig -15°C. Die Wärmeübergänge wurden warmseitig absichtlich etwas niedrig gewählt, nämlich α=5 W/m²K inder Ecke und α=6 W/m²K sonst. Kaltseitig ist α=20 W/m²K.

2.4 Das Computerprogramm

Für die Berechnungen wurde das Computerprogramm STAT3D verwendet, das an der Bundesanstalt für Materialprüfung (BAM) in Berlin entwickelt wurde [1]. Es dient zur Berechnung dreidimensionaler Wärmeströme und Temperaturfelder unter stationären Bedingungen, wobei die Methode der finiten Differenzen verwendet wird. Zum Berechnen und Plotten der Isothermen wurde das Programm ISOSTAT3D gebraucht, das ebenfalls an der BAM entwickelt wurde.

3. RESULTATE

3.1 Temperaturen

Fig. 3: Isothermen zum Fall 9 in Tab. 1

Fig. 4: Isothermen zum Fall 5 in Tab. 1

Die warmseitigen Oberflächentemperaturen werden benötigt, um das Kondenswasserrisiko und die Gefahr von Schimmelpilzbildung zu beurteilen. In einem Raum mit

20°C Lufttemperatur liegt der Taupunkt nach [2] bei 7.7°C, wenn die Aussentemperatur -15°C beträgt.

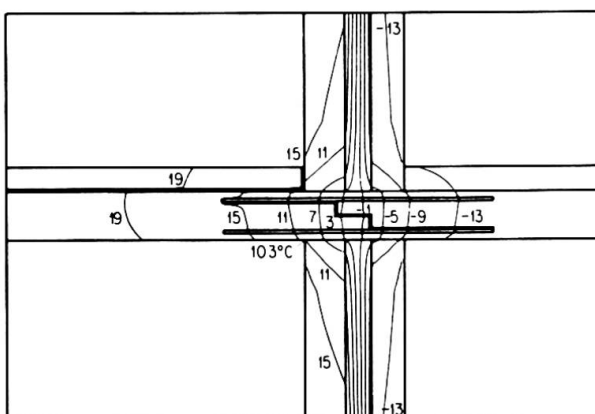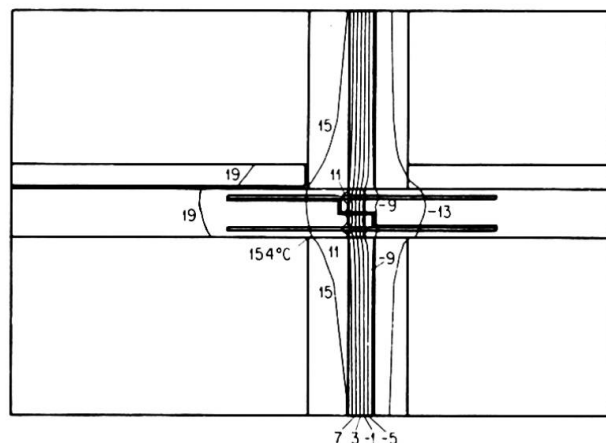Bei der hier berechneten Balkonkonstruktion liegt die tiefste Oberflächentemperatur in der Ecke des unteren Raumes. Sie beträgt im durchbetonierten Fall 10.3°C und liegt damit um 2.6°C über dem Taupunkt. Bereits hier besteht kein Kondenswasserrisiko. Diese Tatsache ist auch auf die gute Wärmedämmung des Zweischalenmauerwerkes zurückzuführen: aus dem Bereich der inneren Schale werden der Betonplatte bedeutende Wärmemengen zugeführt.

Wie Fig. 5 zeigt, liegen mit einem Dämmelement bedeutende Erhöhungen der Oberflächentemperaturen drin. Es ist auffallend, dass die entscheidende Veränderung im Bereich $d/\lambda < 0.4$ m²K/W liegt. Dies bedeutet bei d = 0.06m, dass mit $\lambda = 0.15$ W/mK die entscheidende Verbesserung bereits erreicht ist.

Weiter fällt auf, dass die Verwendung von Edelstahl eine weitere bedeutende Erhöhung der Oberflächentemperatur bewirkt. Ein gutes Dämmelement ergibt gegenüber der durchbetonierten Platte eine Temperaturerhöhung von 2.4°C. Die Verwendung von Edelstahl bringt eine weitere Erhöhung von 2.7°C.

Die mögliche Veränderung des Temperaturfeldes einer Kragplatte wird durch die Isothermen in den Fig. 3 und 4 gezeigt. Man beachte, dass zwei Extremfälle miteinander verglichen werden.

Fig. 5: Tiefste Oberflächentemperatur in Abhängigkeit von d/λ
          Kurve 1: Armierungsstahl   Kurve 2: Edelstahl
          d: Dicke des Dämmelements [m]
          λ: Wärmeleitfähigkeit des Dämmelementes [W/mK]

3.2 Wärmeverluste

Zur Beurteilung der Wärmeverluste, die der Kragplatte angelastet werden müssen, wird ein linearer k-Wert definiert. Er ist ein Mass für die Wärmeverluste pro Meter Kragplattenanschluss. Zu seiner Berechnung wurde der Wärmefluss durch je ein Streifen von 0.75m oberhalb und unterhalb der Kragplatte berücksichtigt.

Der lineare k-Wert ist in Fig. 6 in Abhängigkeit vom Wärmedurchgangswiderstand des Dämmelements dargestellt mit je einer Kurve für Armierungsstahl und Edelstahl. Wie schon bei den Temperaturen stellt sich die entscheidende Verbesserung bei Werten von $d/\lambda < 0.4$ m²K/W ein; die Verwendung von Edelstahl bringt eine zusätzliche drastische Senkung der Wärmeverluste.
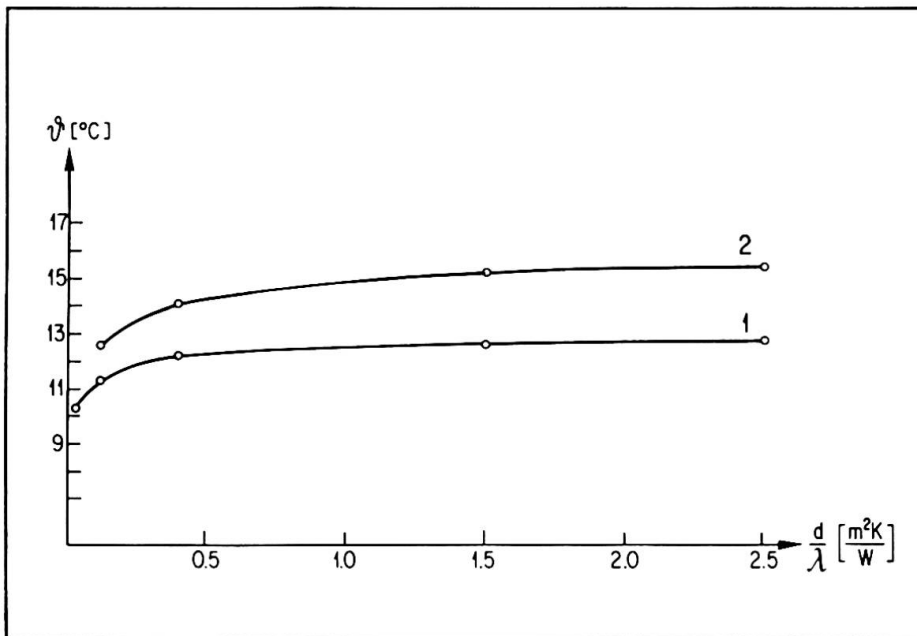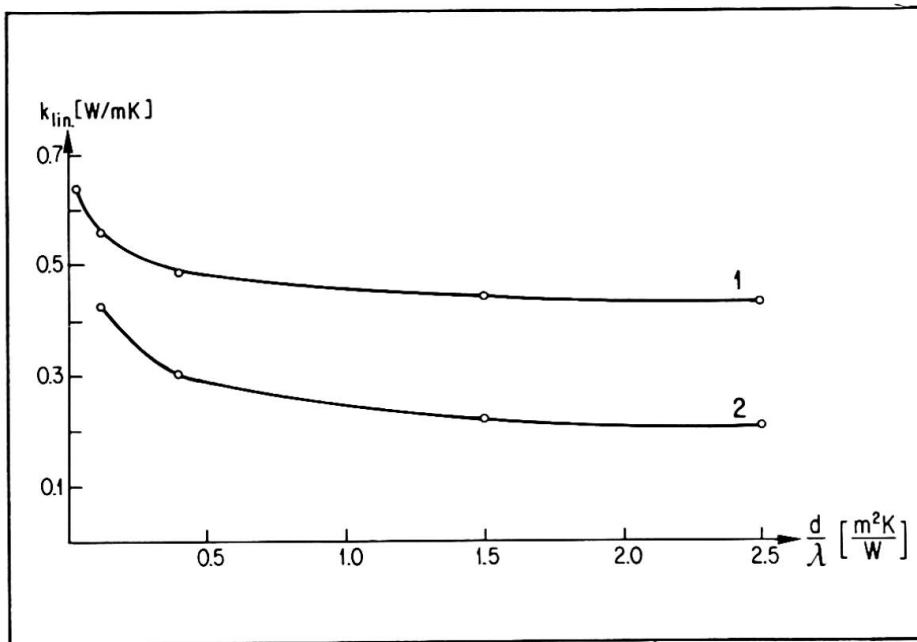
Fig. 6: Linearer k-Wert in Abhängigkeit von d/λ
        Kurve 1: Armierungsstahl   Kurve 2: Edelstahl
        d: Dicke des Dämmelementes [m]
        λ: Wärmeleitfähigkeit des Dämmelementes [W/mK]

Mit Hilfe des linearen k-Wertes und der Heizgradtage lässt sich der Energiever-
lust pro Meter Kragplatte für die Heizperiode abschätzen:

$$E = 24 * k_{lin} * HGT$$

   E: Energieverluste pro Meter Kragplatte während der Heizperiode
   k_{lin}: linearer k-Wert

   HGT: Heizgradtage

Nach [3] ist für die Wetterstation
Zürich SMA HGT = 3616. Für eine
durchbetonierte Kragplatte ergibt
sich damit ein Energieverlust von
56 kWh/ma. Ausgehend von diesem
Basiswert wurden die Energieein-
sparungen berechnet, die mit ver-
schiedenen Dämmelementen und Stählen
möglich sind. Die Resultate sind in
Tab. 2 enthalten.

Fall Nr.	Energieeinsparung [kWh/ma]
1	18
2	17
3	14
4	7
5	38
6	36
7	29
8	19

Tab. 2: Mögliche Energieeinsparungen
        Nummerierung wie in Tab. 1

4. ABSCHLIESSENDE BEMERKUNGEN

Durch Verwendung von Edelstahl bei
Kragplattenanschlussarmierungen las-
sen sich im Bereich des Wärmeschutzes
bedeutende Verbesserungen erzielen.

Gemäss [4] muss darauf hingewiesen werden, dass Edelstahl an Orten, wo Chloride
(Salz) zum Einsatz kommen, korrosionsgefährdet ist. Ein spontanes Versagen der
Konstruktion kann nich ausgeschlossen werden. Armierungsstahl, der im Bereich
der Kragplattenanschlüsse durch Beschichtung vor Korrosion geschützt sein muss,
kündigt ein mögliches Versagen an durch Indizien wie Rostwasser und Neigung der
Konstruktion.

LITERATURVERZEICHNIS

1. RUDOLPHI R., MUELLER R., Bauphysikalische Temperaturberechnungen in FORTRAN. Bd. 1, B.G.Teubner, Stuttgart 1985

2. SIA Empfehlung 180, Wärmeschutz im Hochbau, Schweizerischer Ingenieur- und Architekten-Verein, Zürich 1975

3. SIA Empfehlung 381/3, Heizgradtage der Schweiz, Schweizerischer Ingenieur- und Architekten-Verein, Zürich 1982

4. THEILER F., Korrosion von Stählen, Schweizer Ingenieur und Architekt 7/1986, pp 116

Moisture in Insulated Roofs with Load-bearing Steel Deck

Feuchtigkeit in isolierten Stahldächern

Humidité dans des toitures isolées contenant de la tôle profilée d'acier

Germund JOHANSSON
Assist. Prof.
Chalmers Univ. of Technol.
Göteborg, Sweden

Germund Johansson, born 1937, received his civil engineering degree at Chalmers Univ. of Technology in 1962. After some years at a consulting firm for geotechnical problems he joined the Dep. of Steel and Timber Structures at Chalmers Univ. of Technology. His research interests are, among others, steel structures, roofs, and structural damage (due to snow, wind).

SUMMARY

The paper deals with some practical questions related to roofs and roofing such as moisture, water and melting snow, thermal insulation. Thermal bridges and/or a thick layer of snow can cause melting of the snow. Air transport through the roof and in the roof may cause moisture condensation on the cold surface. Mechanical fasteners need a "dry climate" in order not to corrode.

RÉSUMÉ

L'article traite des problèmes pratiques de toits concernant l'humidité, l'eau et la neige fondue, et l'isolation thermique. Des ponts thermiques et/ou une couche épaisse de neige peuvent provoquer la fonte de la neige. La ventilation dans le toit et à travers le toit peut causer une condensation sur la surface froide. Des attaches mécaniques ont besoin d'un climat sec pour éviter la corrosion.

ZUSAMMENFASSUNG

Einige praktische Probleme mit dem isolierten Stahldach werden beschrieben. Sie betreffen Feuchtigkeit, Isolation, Wasser und schmelzenden Schnee. Schneeschmelze wird bisweilen von Kältebrücken verursacht, aber häufiger von einer dicken Schneeschicht. Lufttransport im Dach und durch das Dach kann Kondensation unter der kalten Oberfläche verursachen. Mechanische Verbindungsmittel brauchen jedoch ein "trockenes Klima", um nicht zu korrodieren.

1. INTRODUCTION

An externally insulated steel deck consists of a load-bearing trapezoidal steel sheet, sometimes a plastic sheeting, thermal insulation and a water proofing layer of roofing felt, a single-ply membrane or steel sheets. Two types are shown in fig.1. The type of roof is very often used in industrial buildings, in schools, in supermarkets etc. Rather thick thermal insulation is used in the roof. This has lead to lower temperature in the waterproofing membrane, which means that the surface will be exposed to larger temperature variations than with a low insulation thickness. This influence may lead to ice cracks in the membrane. To avoid this the membrane must have good flexibility (elastic properties) even at very low temperature and a high elongation at rupture.
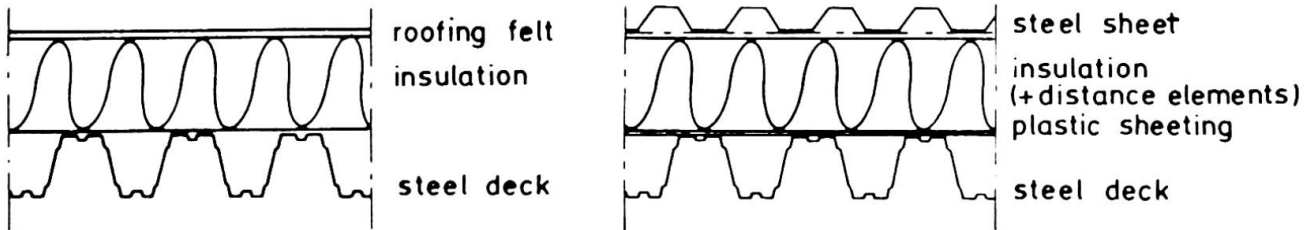

Fig. 1 Two types of insulated steel decks.

2. MOISTRUE

There are several ways for moisture infiltration into the roof. Moisture can be built in during rainy or snowy days. It can get there through leaks in the water-proofing membrane. It can come from the inside of the building through diffusion or convection. Moisture in the structure must have the possibility to disappear from the roof, which means that only one water/air/moisture proof layer is needed. The design with roofing felt on the top and a vapour barrier between the steel deck in the insulation may act as a "moisture trap", fig. 2. Once moisture has entered into such a roof it has to stay there. Diffusion is usually not a problem for the common steel deck and the water built-in usually disappears during the first summer period.

In certain cases convection may cause trouble. If you blow hot humid indoor air into the roof you will get problems. The amount of moisture transported through convection is proportional to the difference in air pressure between the indoor and outdoor air. The steel sheet is airtight – but the splices are not. However, the steel sheet is very often perforated for acoustic reasons and this totally destroys the possibility for the steel deck to prevent the air to enter into the structure.

If, on the other hand, there is no airtight exterior layer, an airtight plastic membrane, "vapour barrier", must be added to the structure, placed between the insulation and the steel deck, cf. fig. 1, or in the insulation placed between two layers of insulation. The plastic membrane is not perfectly tight due to screw penetrations or due to the side overlaps. Measurements show a low amount of air-leak. For a screwhole with remaining screw an air leakage of 0.003 m^3/h has been measured at a pressure difference of 50 Pa. This corresponds to 17 g water during one month if the indoor air has a temperature of 20°C and a 50% relative humidity. When the screw is removed from the hole the air leakage is 0.09 m^3/h per hole, which corresponds to 0.56 kg water per month. The leakage measurements are taken at very high level of the pressure difference. Wind speed and temperature differences may cause 10-20 Pa pressure difference, which is a more realistic level over a longer period of time. With a linear relationship between air leakage and air pressure we only get 5 g moisture per month for each screw.

roofing felt

insulation
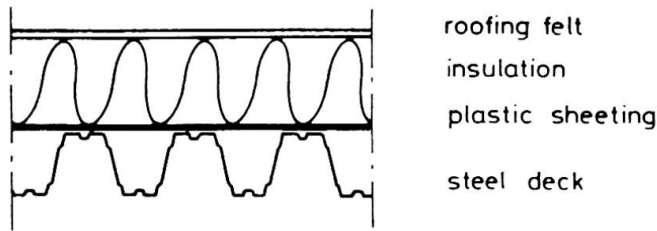
plastic sheeting

steel deck

Fig. 2 Steel deck with two airtight membranes may act as a "moisture trap".

Theoretically and in laboratory tests, but probably not in practice, it is possible to use the steel sheet as an air barrier. Table 1 shows some results from air leakage tests on splices in steel sheet. The sheet was an ordinary trapezoidal steel sheet, 45 mm deep and 0.7 mm thick. The side overlap was riveted with pressure-tight pop rivets. Tests were also conducted with a tightness strip installed in the overlap. The length of the leakage way is 100 mm. The amount of air passing through the joint with the tightness strip is very low. The result is much better than what is usually reached when testing ordinary overlap splices in plastic sheeting.

Humid indoor climate combined with overpressure ventilation may in certain cases lead to problems with condensation in the roof if there is some air leakage through the inner surface. However, "condensation" seems to have become some kind of a general explanation for dripping water, when the leaks are not found after a short and incomplete inspection of the roof.

Table 1 Measured air leakage through pop riveted splices in steel sheet.

Distance between rivets m	Leaking air (m^3/hm) at the pressure difference	
	10 Pa	40 Pa
0.6	0.14	0.51
0.3	0.17	0.58
0.15	0.15	0.56
0.3 (with tightness strip)	0.01	0.04

3. MOISTURE FROM THE OUTSIDE

Sometimes ventilation air coming from the outside may be very dangerous. For a roof with a principal design shown in fig.3 the ventilation air is passing via the space between the upper steel sheet and the thermal insulation. Due to the low temperature of the steel sheet - the roof surface may be 10° C colder than the surrounding outdoor air - the ventilation air will be cooled down. This may lead to condensation in the roof if the temperature is low enough to give 100% relative humidity in the ventilation air. Table 2 shows temperature and humidity measurements for a roof similar to fig.3. The measurements were taken during a clear winter night at different points in the building. There was no snow on the roof.

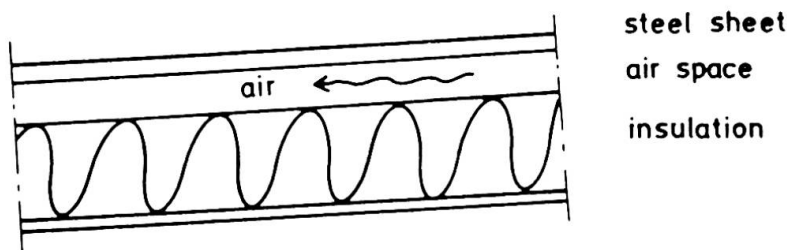steel sheet

air space

insulation

Fig.3 A roof with ventilation air under the exterior steel sheet.

Table 2 Measured temperature and relative humidity for a roof with ventilated exterior steel sheet.

	Temperature °C	Relative humidity %	Moisture content g/m³
Inside the building, near the floor	14.9	24	3.1
Inside the building, near the roof	17.0	25	3.6
In the roof air space, 6 m from intake	-8.0	80	2.0
Outside	-5.0	87	2.8

The results show that both the air tgemperature and the moisture content are lower in the roof than outside. Under certain climatic conditions parts of the roof will act as a giant air dehumidifier. This shows that if there is some moisture in the roof it is not always possible to eliminate it with the aid of ventilation. By increasing the ventilation we may make the situation worse instead of solving the problem.

4.   THE VAPOUR BARRIER AND MECHANICAL FASTENERS

In 1974 in situ investigations of the wind uplift strength of 29 industrial roofs were conducted |1|. All the roofs consisted of a steel deck and thermal insulation (mostly mineral wool) with thickness varying between 40 and 120 mm. On the top there was a bituminous roofing felt. None of the roofs had any type of vapour barrier between the steel deck and the insulation. In 1969 16 of the storm damaged roofs, of the same typ as mentioned above, were investigated |3|. Only one of the 16 roofs had a vapour barrier between the steel deck and the insulation. The use of a vapour barrier was not common for such roofs at that time (only one roof out of 45, i.e. 2%). The insulation and the roofing felt were glued with hot asphalt - no mechanical fasteners were used.

After the heavy storm damages in 1969 a new design philosophy started to grow, and after some years many of the industrial roofs were mechanically fastened with screws and washers. In the beginning the washer was placed directly on the insulation, under the roofing felt. After some blow offs the washers were applied after the first layer of roofing felt had been glued to the insulation. Since then there have not been any problems with blow offs if the work was carried out properly and if the design was correct. Some years after the introduction of mechanical fasteners the risk of corrosion on the fastener became a question of interest. Therfore, in 1979-1980 the fasteners on 14 different roofs (steel deck, insulation, roofing felt) were investigated by J Hellgren and B Johansson |2|. The oldest roofs that could be found were selected - the oldest roof investigated was eight years old and without any signs of corrosion. A total of 134 screws + washers have been removed and examined. The average age of the roofs was 5 years. Some little rust was found on 5% of the examined screws, but no serious corrosion was found. In Norway a similar investigation has been made in 1985 |4|. Forty-eight roofs have been examined, conrete, wood and steel roofs. The steel deck roofs can be separated into two types, roofs with and without vapour barrier respectively. The roofs with a vapour barrier show rust on the screw or washer in eight roofs out of nine. On the other hand, the roofs without a vapour barrier show red rust for one single screw on nine roofs.

These two investigations show that omitting the vapour barrier will not ruin the roof if there is an airtight membrane (roofing felt, PVC, EDM etc) as a top layer. Instead, the vapour barrier may be destructive for the roof. Usually there is no need for a vapour barrier if there is a roofing felt on the top. This type of roof has behaved well for a long time.

5.   SNOW ON THE ROOF

During the winter time, when there is snow on the roof, we sometimes get a zone
of melting snow close to the roof membrane. Some engineers - and that is not
just a few - believe that the melting snow is caused by thermal bridges through
the roof insulation. This may sometimes be the right explanation but more com-
monly the explanation is much simpler. The snow on the roof functions as an addi-
tional exterior thermal insulation. The snow temperature can never exceed $0^{\circ}C$
which limits the effect of its thermal insulation properties. Due to the insula-
tion effect of snow the zero temperature zone will be in the snow layer under
certain circumstances. As long as the temperature on the top of the roof is $0^{\circ}C$
the heat flow through the roof is constant.

For a roof consisting of a load-bearing steel deck, thermal insulation, water
proofing membrane and a layer of snow, the temperature between the membrane and
the layer of snow can be expressed as

$$\theta = \theta_e + \frac{R_{s,e} + d_{snow}/\lambda_{snow}}{R_{s,e} + R_{s,i} + R + \frac{d_{snow}}{\lambda_{snow}}} (\theta_i - \theta_e) \qquad (1)$$

where

θ = temperature at the membrane λ_{snow} = thermal conductivity for snow
θ_e = exterior temperature R = thermal resistance
θ_i = interior temperature d_{snow} = snow thickness
$R_{s,e}$= thermal resistance for the exterior surface (0.04 m^2 $^{\circ}$C/W)
$R_{s,i}$= thermal resistance for the interior surface (0.13 m^2 $^{\circ}$C/W)

The snow on the roof will start to melt when the temperature θ at the membrane
equals zero. From equation (1) we obtain the minimum snow depth at which the snow-
melting starts.

$$d_{snow}/\lambda_{snow} = R_{s,e} + (R + R_{s,i})(-\theta_e)/\theta_i \qquad (2)$$

In the diagram, fig. 4, relationships between temperature and snow depth are
given for different values of the thermal conductivity for snow. The example in
fig. 4 consists of 200 mm mineral wool with $\lambda = 0.040$ W/m $^{\circ}$C and the temperature
indoor is 20 $^{\circ}$C. The relationship between the thermal conductivities for snow
used in the diagram and the density of snow are approximately

λ_{snow}(W/m $^{\circ}$C)   : 0.05   0.10   0.20
density (kg/m^3) : 100   200   300

The density 100 kg/m^3 corresponds to new powder snow and the density 300 kg/m^3 is
used in different codes to determine the snow load on the roof. From fig. 4 it
can be seen that new powder snow very soon starts to melt. If the outside tempera-
ture is $-3\,^{\circ}$C the snow will start melting at 40 mm thickness. The older snow with
300 kg/m^3 density will start melting at 260 mm snow depth if the outside air tem-
perature is -5°C.

The melting snow due to thermal insulation properties of the snow may explain
many odd things, e.g. why water is dripping from the roof although the tempera-
ture is pretty much below the freezing point, why there nearly always is a
layer of ice between the layer of snow and the membrane, why water sometimes
enters into the structure even when it is cold outside. Melting snow on the roof
is a quite normal physical phenomenon and it does not necessary indicate any
faults in the design. As there is a temperature variation between day and night
there will be periods of melting and freezing. This may have a bad influence on

the water-proofing membrane, perhaps with cracks and water leaks. Mechanical fasteners act as thermal bridges and contribute to the melting of the snow. This may be seen in frosty autumn mornings. The energy transport through the fasteners is very small. One screw ($\emptyset$ = 4 mm) per m^2 only gives an increase of the U-value of approximately 0.003 W/m^2 ^oC. The interior temperature and the
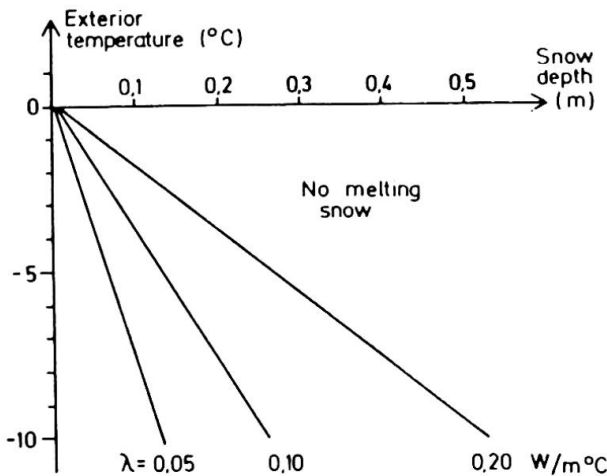

Fig. 4   Relationship between exterior temperature and snowdepth on a roof with R = 0.2/0.004 = 5 m^2 ^oC/W. Interior temperature is 20^oC.

thermal resistance of the roof limits the amount of energy transportation through the roof. In order to melt one kg ice 334$\cdot 10^3$ Ws is required. With a thermal resistance of 5.13 m^2 ^oC/W and a 20^oC difference in temperature it takes 23.8 hours to melt 1 kg snow. With a snow density of 200 kg/m^3, 5 mm depth corresponds to 1 kg/m^2. With the presumptions used it takes about three weeks to melt 100 mm snow. Some of the water in the melting zone will run away and some will remain in the snow on the roof. It is this blend of water and melting snow that may leak through or create problems for the membrane if the temperature falls.

6.   CONCLUSIONS

Make the membrane ductile enough to withstand ice on the roof - then, together with good workmanship, the risk of leaking water is minimised.

Don´t force humid indoor air into the roof - don´t use overpressure ventilation, use underpressure ventilation instead. The vapour barrier may be punched through and in that case over pressure ventilation is not suitable. Increased ventilation in the roof may not be the solution of a moisture problem; instead it may make it worse. It all depends on the physical causes.

REFERENCES

1. GULLBRANDSON B. - JOHANSSON G., Field investigation of externally insulated sheeting roofs. Document D15:1978. Swedish Council for Building research.

2. HELLGREN J. - JOHANSSON B., Field tests of mechanical fasteners in externally insulated steel decks. (In Swedish). Int. paper S80:1. Division Steel and Timber Structures. Chalmers Univ of Technology, Göteborg 1980.

3. JOHANSSON G., Storm damage in Western Sweden. (In Swedish). Report R33:1970 Swedish Council for Building research.

4. PAULSEN E., Roofing fasteners. Report 21. Norwegian Building Research Institute, Trondheim 1987.

Environmental and Social Aspects of Large-Panel Technology in Housing

Aspects sociaux et d'environment de la technologie dans le bâtiment

Ökologische und soziale Probleme der Grossplattenbauweise im Wohnungsbau

Jan AUGUSTYN
Professor
Warsaw, Poland

J. Augustyn, born 1921, received his civil engineering degree at the Silesian Technical University in Gliwice. He worked in design offices and research centers dealing with civil engineering structures. Now he is a professor at Technical University in Częstochowa.

Jerzy A. POGORZELSKI
Professor
Warsaw, Poland

J. A. Pogorzelski, born 1939, received his civil engineering degree at Technical University of Warsaw. Since 1960 he works in Building Research Institute dealing with problems of building physics and fire safety of buildings.

SUMMARY
The paper deals with non-structural problems arising in large-panel dwelling houses in Poland during the past 25 years. Many unfavourable consequences in technical, environmental and social aspects have already occurred. The state of the art, measures of prevention and concepts of improvements being applied nowadays in Poland are reported.

RÉSUMÉ
Le rapport traite des problèmes non structuraux apparus en Pologne pendant les 25 dernières années dans les maisons d'habitation préfabriquées. Un grand nombre de conséquences néfastes s'est déjà manifesté dans le domaine technique, d'environnement et social. L'état de la science, les mesures de précaution et les concepts d'amélioration appliques à présent en Pologne, sont présentés.

ZUSAMMENFASSUNG
In dem Beitrage wird über die nicht-konstruktiven Probleme der Grossplattenbauweise im Wohnungsbau Polens der letzten 25 Jahre berichtet. Dazu gehören zahlreiche ungünstige Folgen von technischer, ökologischer und sozialer Bedeutung. Der aktuelle Stand dieser Probleme sowie die Konzepte der in Polen bisher vorgenommenen Verbesserungsmassnahmen werden dargestellt.

1. INTRODUCTION

Severe destruction of housing substance in Poland during World War Two as well as mass migration of people from the countryside into towns necessitated building many dwelling houses as quickly as possible. In Poland and most other east-European countries the large-panel technology of construction has been developed on a very large scale. This technology seemed to be very promising for solution of housing problems with respect to:
- location of most of building operations in factories and making them irrespective of weather conditions,
- assurance of higher quality in industrial processes,
- stable and regular supply of structural components partially stored in buffer stores.

On the basis of these assumptions the large-panel system has become very widespread and nearly the sole technology in Poland for dwelling houses. About 200 industrial plants for prefabrication of large-panel buildings have been assembled and from their production about 100 000 flats are constructe every year.

Such monoculture of building technology has been found to cause many unfavourable consequences in technical, environmental and social aspects that deeply influence the life conditions of inhabitants. Particular aspects of such influence are discussed below.

The illustrations /drawing, photos/ will be shown during presentation of the paper.

2. SOCIAL AND ENVIRONMENTAL ASPECTS

2.1. Social and family life aspects

In multi-storey dwelling houses being erected nowadays in Poland the area of individual flats is subject to limitations defined in administrative rules and depends upon number of inhabitants. On the other hand the time of expectation for a flat extends up to 15...20 years and tends to prolong. Therefore many families live in flats much too small for their needs /two or three generations instead of one/ whereas some old people can not afford to pay the rents for their relatively too big flats. An exchange of flats is often hampered by bureaucracy. In the mid 70-ties the attempts of seeking the technical solutions of division or joining of flats were made with practically no success.

Too small area of most dwellings and needs for privacy in overcrowded flats do not contribute to looking for the adjustment of lay-out by demolishing or replacement of partitions within flats. Even light-weight honey-comb gypsum boards used instead of concrete slabs or masonry walls do not tempt the residents to change the lay-out; they are often replaced by masonry partitions as giving better acoustical and functional solutions.

The problem of inflexibility of large panel buildings arises too in the scale of town planning. The use of heavy cranes for erection of large-panel buildings tends to limit location of new settlements on open grounds outside the existing town. The unified dimensions of panels and differences of desired room heights do not allow to accomodate the dwelling and the shops in the same building. Dwelling houses spread out for better exposure to Sun as well for location of parking places and children playing grounds do not form streets or squares attracting people to walk or to gather.

The disappearance of traditional streets, alleys and squares makes the social contacts and bonds poorer and brings the feeling of isolation and depression. As the new residential areas are poorly equipped with kindergartens, schools, shops, cultural centers and hospitals, the whole productive and cultural activity of inhabitants is performed in the city. The humanisation of new building areas can be achieved only by differented architecture and "saturation" of new districts with social and cultural facilities making them vivid and attractive. Few attempts have been hitherto succesful.

In many small towns new large-panels blocks do not harmonise with existing architecture and social tissue; they dominate the town and destroy social bonds. Deformation of a landscape by heavy large-panel buildings is a special form of architectural pollution, especially in small towns with their graceful old architecture or in a health resort situated in a beautiful landscape.

2.2. Acoustical aspects

The level of acoustical requirements in the relevant Polish Standard conforms to mean world standards. Characteristic features of dwelling houses erected in Poland after World War Two /multi-family houses prevailing, large-panel buildings, small area and overcrowding of flats/ create however special problems. Despite of sufficient thickness of heavy concrete walls /14...15 cm/ and floors /14...16 cm/ about 30...50% of inhabitants complain of noise from upper stories and about 10...20% complain of noise from neighbouring flats on the same storey. The main reasons of this state are:

- good transmission of noise through concrete,
- acoustical bridges in places of joints and openings in concrete slabs,
- poor insulation of service pipes,
- no possibility of proper insulation and dilatation of technical rooms in large-panel buildings,
- poor quality of construction,
- poor acoustical quality of installation equipment.

A separate problem is the traffic noise as the density of traffic increases. The noise protection should be achieved by:

- proper town planning,
- proper lay-out of the building itself,
- sufficient acoustical insulation of external walls including windows.

Two first means are very rarely respected in town-planning and architectural design. Windows of increased acoustical insulation are not always used according to the need. There are not windows available of high acoustical insulation and of controlled air input rate.

Generally there is no technical supervision and inspection of completed buildings from the acoustical point of view. Nobody checks the conformance of buildings with acoustical requirements prescribed by relevant standard. The measurements are conducted sporadically, only in cases of frequent complaints.

2.3. Heat and moisture aspects

Heat insulation requirements were introduced to the relevant Polish Standard since 1957 /for outer walls k-value below 1 kcal/m^2h^oC, for flat roofs below 0,75 kcal/m^2h^oC/ on the basis of long-term previous experience with masonry walls. This coresponded with

red brick wall, two bricks thick, both sides plastered /total
thickness approx. 55 cm/. Long-term experience has shown quite
good performance of such walls in the moderately-cold climate of
Poland.

The same requirements applied to the multi-layered walls of large
concrete panels have proved to be unsatisfactory. There are many
cases of condensation on the cold bridges /insulation voids, cor-
ners of walls, horizontal joints/, combined sometimes with rain
water leaks through the joints or cracks in outer cladding. Due
to cold bridges caused by improper design or fabrication faults
usually real k-value exceeds by 20...40% the nominal k-value. Up
to now this effect is not taken into consideration in design prac-
tice and in Polish Standards. It results in too small area of ra-
diators installed.

Almost all dwelling houses with large pan ls have heat supply from
heating plants or district power plants. No local thermostats are
used, there is only central regulation of heating medium accord-
ing to the outside air temperature. Distant heating lines are usu-
ally in bad condition due to corrosion; heat losses including the
hot water leaks reach up to 18...20%. Failures in heat supply con-
cerning single houses or even whole districts occur relatively of-
ten. As a result a large portion of dwelling houses are tempora-
rily or permanently poorly heated, while some of the others are
over-heated.

Natural ventilation is a prevailing system in dwelling houses up
to 12 storeys with its efficiency time and place dependent. The
residents of poorly heated dwellings often close the inlets to the
ventilation flues in order to diminish the heat losses, increasing
in such a manner the relative humidity of air. The increase of re-
lative humidity is often caused by the overcrowding of dwellings
/e.g. small flats occupied by people with small children/. The
lack of space and sometimes architectural solutions often force
people to place the pieces of furniture /beds, cupboards, book-
shelves/ at the outer walls, stopping the convective streams. It
results in a surface condensation.

Since 1982 the house owners /building co-operatives/ can get remit-
ted credit for execution of additional cladding or additional in-
sulation of outer walls if technological faults occur. At the same
time heat insulation requirements for new buildings were heighten-
ed /k-value for outer walls should not exceed 0,75 W/m²K/.

Some thousands of houses have been already additionally insulated
either with glued expanded polistyrene or with mechanically fixed
mineral wool slabs. It resulted in improving the comfort condit-
ions with no heat saving effect as no regulation of heating sys-
tem has been performed.

For the time being the complex program of energy saving is under
preparation. In 1989-92 successively maximum k-value for outer
walls will be changed to 0,35...0,45 J/m²K, for windows to 2 W/
m²K. The radiators will be equipped with thermostatic walves, air-
tightness of windows will be improved. There is a tendency to
reach zero-growth of energy consumption at about 2000...2005. It
means the necessity for thermo-renovation most of the existing
buildings, including the introduction of controlled mechanical
ventilation.

2.4. Microbiological environment contamination

Insufficient thermal insulation of external envelope, the faults

of central regulation and heat supply, random efficiency of natu-
ral ventilation, over-crowding of dwellings - form beneficial con-
ditions for the growth of micro-flora. The problem has been exten-
sively studied since late 70-ties by several research centers.
In buildings of concrete panels mostly mould fungi occur as a com-
pound of micro-flora. Such materials like floorings with base of
natural fibres, wall papers, paints, glues, lignocellulose mater-
ials - are especially vulnerable to biocorrosion. The measurements
performed by Building Research Institute have shown, that build-
ings with outer walls attacked by mould are highly polluted by
fungi spores /mostly Penicillium, Aspergillus and Cladosporium/.
The spores can cause allergy and different sicknesses, mostly of
air passages and lungs. The best way of counter-action against
micro-flora growth is to eliminate high moisture content in mate-
rials, caused mostly by condensation. The additional insulation
of the external envelope, good ventilation and required heat sup-
ply eliminate the ground for fungi.
Due to the great number of buildings "waiting" for thermorenovat-
ion the chemical means of mould control have been used, too. Many
of them, however, had to be withdrawn from use due to emission of
toxic gases.

2.5. Chemical pollution of air

Chemical pollution of air with toxic or allergic gases occurs ve-
ry often due to use in construction of such materials as: impreg-
nates, tar, adhesives, paints and lacquers, chemo-hardening plas-
tics, organic solvents. The most often found compounds are phenol,
formaldehyde and chlorophenols. The main sources of emission are
usually:
     - as concerns phenol and chlorophenols - insulation hardboards
used in floor layers impregnated with "Xylamite", mineral wool
slabs, tar and tar roof felt, adhesives and furniture of wood par-
ticles slabs,
     - as concerns formaldehyde - furniture, chemo-hardening lac-
quers and adhesives.
Nowadays use of many "suspected" materials is under the control of
health inspection.

2.6. Natural radio-activity of building materials

The first pilot investigations were started at the end of 60-ties.
Since the mid 70-ties the ground has been laid for mass control
investigation of natural radiation /methods, apparatus, criteria
and qualified staff/. Since 1980 the control of natural radiation
of some "suspected" materials has become obligatory. On the basis
of past results as such materials can be treated: aerated concret-
es on the basis of fly-ashes, furnace slag concrete, ceramic brick,
cement with admixture of fly-ashes. The use of these materials
should be permanently controlled and materials with high natural
radioactivity should be mixed with neutral materials or eliminat-
ed. The Polish Standard determining allowable concentrations of
radioactive elements in building materials is under preparation.

3. CONCLUSIONS

General circumstances after World War Two substantiated the large-
panel technology of construction which contributed in reconstruct-
ion of destroyed towns and cities. This technology was applied on
a very large scale and for a long time as the predominant system

of construction has been proved, however, to cause many unfavour-
able consequences for the internal as well as the external envi-
ronment of buildings, resulting in a deterioration of the living
conditions of inhabitants. The authors, coming to this conclusion
realize that not all the problems can be attributed solely to
the large-panel system of construction and they will not be solv-
ed by a simple change of construction system which is only one of
many factors influencing the environment and living conditions.

Leere Seite

Blank page

Page vide

Leere Seite

Blank page

Page vide